DICAL Indonesia.
Marine Res. in Indonesia

PENJELIDIKAN LAUT DI INDONESIA

MARINE RESEARCH IN INDONESIA

No. 2

The computation of oceanic and meteorological fields of motion with friction proportional to the velocity

by

KLAUS WYRTKI

Surface salinities in the Strait of Malacca

by

RD. E. SOERIAATMADJA

Oceanographic Station List 1956

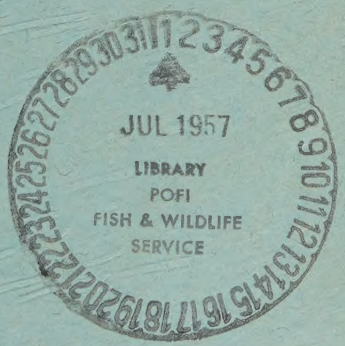

Djakarta 1956

LEMBAGA PENJELIDIKAN LAUT — INSTITUTE OF MARINE RESEARCH

PRINTED BY ARCHIPEL, BOGOR
1956

NOTICE.

The Journal PENJELIDIKAN LAUT DI INDONESIA - MARINE RESEARCH IN INDONESIA appears in irregular intervals. It contains scientific articles and observation results concerning marine research in Indonesian and adjacent waters as well as problems of general interest out of the work of the Lembaga Penjelidikan Laut - Institute of Marine Research.

The journal is available in exchange as well as for purchase by the central library Bibliotheca Bogoriense, Djalan Raya 20, Bogor, Indonesia.

Correspondence concerning the journal should be directed to the head of the Lembaga Penjelidikan Laut, Pasar Ikan, Djakarta-Kota, Indonesia.

Price 1 US-Dollar

THE COMPUTATION OF OCEANIC AND METEOROLOGICAL FIELDS OF MOTION WITH FRICTION PROPORTIONAL TO THE VELOCITY

by

KLAUS WYRTKI

SUMMARY

The friction in the hydrodynamical differential equations is taken proportional to the velocity. With it simple relations result, permitting the calculation of the mass transport, without the need to solve differential equations, if the wind and pressure distributions are known. The solution can cross the equator freely. Simultaneously the equations give the vertical components of motion at the lower boundary of the layer under consideration. Numerical values of the friction coefficient are given, and oceanographical and meteorological models are discussed, as for instance the monsoon winds over Southeast Asia, the monsoon currents in the Java and China Seas and the equatorial currents of the Pacific Ocean.

ZUSAMMENFASSUNG

Die Reibung wird in den hydrodynamischen Differentialgleichungen proportional der Geschwindigkeit angesetzt. Damit ergeben sich einfache Beziehungen, die es gestatten, bei Kenntnis der Wind- und Druckverteilung die Massentransporte zu berechnen, ohne Differentialgleichungen lösen zu müssen. Die Lösungen können den Äquator beliebig überschreiten. Gleichzeitig liefern die Gleichungen die vertikalen Bewegungskomponenten an der Unterkante der betrachteten Schicht. Angaben über die Grösse des Reibungskoeffizienten werden gemacht und Beispiele aus der Meteorologie und Ozeanographie werden diskutiert, so die Monsunwinde über Südostasien, die Monsunströmungen in der Java- und China- See und die äquatorialen Strömungen im Pazifischen Ozean.

ICHTISAR

Gesekan dalam perbandingan-perbandingan diferensial hydrodinamis, diperoleh sebanding dengan ketjepatan. Dengan hasil perhubungannja jang sederhana, memungkinkan perhitungan dari pemindahan setjara masal, tidak usah membutuhkan pemetjahan dari perbandingan-perbandingan diferensial itu, apabila peredaran angin dan tekenan telah diketahui. Pendapatan itu dapat melintasi chatulistiwa dengan bebas. Bersamaan dengan itu perbandingan-perbandingan tersebut memberikan bagian-bagian gerakan setjara menegak dibatas bawah daripada lapisan jang dimaksud. Beberapa nilai dari koëfisiën gesekan telah diberikan dan model-model oceanografis dan meteorologis telah dikupas, misalnja mengenai angin musim di-Asia Tenggara, arus musim di-Laut Djawa dan Laut Tiongkok dan arus chatulistiwa dari Lautan Teduh.

Introduction

In physical oceanography the determination of the field of motion is most importend, but also most complicated. Its determination requires the observation of a three-dimensional vector field, variable also in time, which is naturally most difficult. Therefor the possibilities of its direct determination are limited, and one often changes to indirect methods which permit obtaining results on the distribution of velocity. On the one hand, one can turn back to scalar fields, the distribution of density and pressure, or one can use the boundary conditions, the distribution of the stress of wind, of which a detailed observation is possible. From these, the field of motion can be derived by means of the hydrodynamical differential equations.

In recent years there has been a step forward in considering the topography of the sea level to be primarily an effect of the wind, so that it becames possible to derive the whole circulation from the distribution of wind stress only. But this assumption neglects the fact that water masses of different densities are formed in the different climatic regions, which must produce currents at their boundaries. The formation of specific water masses leads to a continuous increase of the potential energy in certain regions of the oceans. The exclusive use of the distribution of wind stress for the determination of the motion and of the topography of the sea level leads to partial differential equations, which on principle can be solved, if the necessary boundary conditions are given.

The boundary conditions are trivial, if the circulation takes place in a completely enclosed basin, because they are based on the physically logical assumptions that at the boundary the normal component of the velocity and its derivation must vanish. For such enclosed basins the differential equation gives solutions, showing the gross features of the circulation in relatively good agreement with the observations, as modern investigations have shown.

If, on the other hand, a solution is required for a region not enclosed by natural boundaries, the boundary conditions must be observed. But to avoid this was the primary purpose for the application of these theories, because the assumptions which must be made in the case of a region which is not enclosed, are mostly so fareaching that they anticipate the solution. The real deficiency of these theories is that their application is limited to completely enclosed basins and can be used only definitly for the treatment of oceanographical observations in limited regions.

Because the consideration of the stress of wind is equivalent to a continuous addition of energy to the ocean, it is necessary to make use

of the dissipation terms in the hydrodynamic equations. Presently this is done in two different ways, using the diffusion of the impulse, which leads to the coefficients of horizontal A^h and vertical A^v eddy viscosity, or taking the friction R proportional to the velocities, $R = r\,v$, as common in hydraulics. The use of A^h and A^v leads to differential equations of relative high order, moreover the coefficients themselves are determinated only insufficient and depend on the size of the movements under consideration. A view on the tables given by SVERDRUP (1946) for A^h and A^v shows how unsatisfactory calculations must become, using these coefficients. On the other hand the use of the linear friction coefficient simplifies the treatment of the hydrodynamical equations, especially in the case of numerical calculations, as shown by HANSEN (1951). But values of the friction coefficient r are not yet known accurately enough and must be determinated. This paper shall be a contribution in this direction.

Theory. The investigations are basing on the hydrodynamical differential equations in the form

$$\begin{aligned} \varrho\, f\, v + A^h \triangle u + A^v u_{zz} - p_x &= 0 \\ -\varrho\, f\, u + A^h \triangle v + A^v v_{zz} - p_y &= 0 \\ p_z &= \varrho\, g \\ u_x + v_y + w_z &= 0 \end{aligned} \tag{1}$$

Therefor it is assumed that the movements are stationary, that the inertial terms can be omitted, and that the vertical movements are of importance only for the equation of continuity. ROSSBY (1936) has shown for the Gulf Stream that it is not always possible to drop the nonlinear terms, especially not in regions with high velocities and velocity gradients. There are u, v, w the components of the velocity in x, y, z- direction, respectively, ϱ the density, g the acceleration of the earth, $f = 2\,\omega \sin \varphi$ the coriolis parameter, A^h the horizontal and A^v the vertical eddy viscosity and $\triangle$ the Laplace operator. The x-axis points eastward, the y-axis northward and the z-axis positive down.

Integrating this system from the surface to the depth D, about which restrictions need not yet be made, and assuming that

$$\int_0^D \varrho\, u\, dz = M^x \quad \text{and} \quad \int_0^D \varrho\, v\, dz = M^y \tag{2}$$

are the components of the mass transport M, and that

$$(A^v u_z)_0 = -\tau^x \quad \text{and} \quad (A^v v_z)_0 = -\tau^y \tag{3}$$

are the components of the wind stress τ, which can be assumed to be known, the system (1) becomes

$$
\begin{aligned}
f M^y + \frac{A^h}{\varrho} \triangle M^x + (A^v u_z)_D + \tau^x - P_x &= 0 \\
-f M^x + \frac{A^h}{\varrho} \triangle M^y + (A^v v_z)_D + \tau^y - P_y &= 0 \\
P = \int_0^D p \, dz \quad / \quad p &= \int_0^z \varrho \, g \, dz \\
M_x^x + M_y^y &= - \varrho \, w_D
\end{aligned}
\tag{4}
$$

Only in the special case that there are no vertical movements in the depth D, the divergence of mass transport vanishes. Combining the terms representing the friction, and assuming them to be proportional to the mass transport M, it is

$$
\begin{aligned}
\frac{A^h}{\varrho} \triangle M^x + (A^v u_z)_D &= - r \, M^x \\
\frac{A^h}{\varrho} \triangle M^y + (A^v v_z)_D &= - r \, M^y
\end{aligned}
\tag{5}
$$

and r is the friction coefficient. The friction consists of two terms, the internal friction, represented by the horizontal eddy viscosity, and the boundary friction in the depth D. From this it follows that the coefficient of friction will depend on whether or not the velocity gradient in the depth D vanishes. The zero-layer, used by DEFANT (1941) in the Atlantic Ocean has been chosen in a depth where the vertical gradient of the horizontal velocity vanishes, and it has been assumed that in that depth the horizontal velocity itself vanishes. Using such a depth, the coefficient r must become extremely small. It would be quite different if D is the bottom of a shallow sea, because than the bottom friction might be the predominate factor, and r would become relatively large. Introducing (5) into (4) the system (1) becomes

$$
\begin{aligned}
-f M^y + r M^x &= \tau^x - P_x \\
f M^x + r M^y &= \tau^y - P_y \\
P = \int_0^D p \, dz \\
M_x^x + M_y^y &= - \varrho \, w_D
\end{aligned}
\tag{6}
$$

This system of equations gives M as a function of the distribution of wind stress and pressure. P is to be calculated from the distribution of mass.

Because the topography of the sea surface is essentially affected by the winds, in the last years the attempt has been made to present the mass transport M as a function of the wind stress τ alone, STOMMEL (1948), MUNK (1950), HIDAKA (1950 and 1955), HANSEN (1951). A stream function ψ is introduced with

$$M^x = \psi_y \text{ and } M^y = -\psi_x$$

This leads necessarily to

$$M^x_x + M^y_y = 0 \text{ and } w_D = 0$$

It follows that, in the case of the introduction of a stream function, D must be a depth in which the vertical movements vanish. This has been pointed out by HANSEN (1951), but in his calculations for the equatorial parts of the Atlantic Ocean he does not use this restriction. Already in a depth of 200 m he assumes these movements to play an unimportant role which, however, is not confirmed. HIDAKA (1955), on the other hand, has derived from a similar equation the divergence in the upper 100 to 200 m of the Pacific Ocean, and obtains considerable values, the distribution of which is in fair agreement with the observations. Also NEUMANN (1954) does not consider this necessary when using for D the zero-layer of DEFANT (1941). Probably a considerable vertical transport takes place through this layer, which has been made plausible by WÜST (1950), discussing the general circulation of the Atlantic Ocean.

Cross differentiation of (6) and use of the stream function ψ gives the differential equation

$$f_y \psi_x + r \Delta \psi = \tau^x_y - \tau^y_x \quad \text{for } D = \text{const.}$$

Also a variable D can be considered, as done by NEUMANN (1954), but in every case it is necessary that in the depth D the vertical movements vanish. That is always satisfied if D is the very bottom. This equation permits the determination of the stream function, as well as of the topography of the sea level. This can be done analytically or numerically as done by HANSEN (1951) for the Atlantic Ocean.

An alternate method can be used if, beside the distribution of the wind stress, the distribution of pressure resulting from hydrographic observations is assumed to be known. In this case the system (6) can be solved directly for M^x and M^y and gives, moreover, the vertical velocity w_D in the depth D. For investigations which do not concern a totaly enclosed basin, but only a part of the ocean, this might be an advantage. Moreover, it is not necessary to solve a differential equation. In most of these cases it will be possible to choose the depth D in such a way that

the density ϱ is constant within D. Than the system of equations becomes very simple. The pressure p is given as a function of z, $p = \varrho g\ (z + h)$, where h is the topography of the sea level.

$$
\begin{aligned}
-f M^y + r M^x &= \tau^x - \varrho\ g\ Dh_x \\
f M^x + r M^y &= \tau^y - \varrho\ g\ Dh_y \\
P &= \varrho\ g\ D\ (\tfrac{D}{2} + h) \\
M^x_x + M^y_y &= -\varrho\ w_D
\end{aligned}
\tag{7}
$$

The elimination of M gives

$$
\begin{aligned}
(f^2 + r^2)\ M^x &= r\ \tau^x + f\ \tau^y - r\ \varrho\ g\ Dh_x - f\ \varrho\ g\ Dh_y \\
(f^2 + r^2)\ M^y &= r\ \tau^y - f\ \tau^x + f\ \varrho\ g\ Dh_x - r\ \varrho\ g\ Dh_y
\end{aligned}
\tag{8}
$$

and shows the components of the mass transport as a function of the components of the wind stress and of the slopes of the sea level. The solution can cross the equator without becoming infinite. Because a stream function is not used, it is not necessary that div M = O, and the equations (7) permit calculating the divergence of the layer D.

At oceanic models, where the wind stress differs from zero, the equations (7) always give the mass transport M, or at constant density the volume transport V. At meteorological models it becomes possible to divide by D, which gives a simple system, with only the components of the velocities and the atmospheric pressure.

$$
\begin{aligned}
-f v + r u &= \frac{1}{\varrho}\ p_x \\
f u + r v &= \frac{1}{\varrho}\ p_y \\
u_x + v_y &= -w_z
\end{aligned}
\tag{9}
$$

The friction coefficient r. Before further investigations it becomes necessary to study the numerical values of the coefficient r and the basic properties of the equations (8). For this purpose they can be written in the form

$$
\begin{aligned}
r M^x - f M^y &= K^x \\
f M^x + r M^y &= K^y
\end{aligned}
\tag{10}
$$

where the components of the stress K are given by

$$K^x = \tau^x - \varrho\ g\ Dh_x \qquad \text{and} \qquad K^y = \tau^y - \varrho\ g\ Dh_y$$

Then equation (10) combines the vector of the mass transport M with the vector of the stress K. Elimination of M gives

$$
\begin{aligned}
M^x &= \frac{1}{f^2 + r^2}\ (r K^x + f K^y) \\
M^y &= \frac{1}{f^2 + r^2}\ (r K^y - f K^x)
\end{aligned}
\tag{11}
$$

Introducing

$$K^x = K \cos \beta \qquad \text{and} \qquad M^x = M \cos \gamma$$
$$K^y = K \sin \beta \qquad\qquad M^y = M \sin \gamma$$

a simple calculation gives

$$M = \frac{K}{\sqrt{f^2 + r^2}} \tag{12}$$

$$\cos (\gamma - \beta) = \frac{-r}{\sqrt{f^2 + r^2}} \tag{13}$$

Because r never becomes zero, M is defined also at the equator. The expression (12) combines the magnitude of the mass transport M or of the velocity c with the stress K. In geostrophic currents $M = \frac{K}{f}$, where K must become zero at the equator and the mass transport would be indeterminated. The function $\frac{1}{\sqrt{f^2 + r^2}}$ is represented in Fig. 1 for different values of r as a function of latitude. The curve r = O corresponds to geostrophic currents. It is apparent that the influence of the friction is especially remarkable in the vicinity of the equator. At small friction, $r < 2.10^{-5}$ sec^{-1} the curves approximate closely the curve for r = O and deviate only in lower latitudes. At higher friction the function is relatively independent of latitude.

The angle between the vector of the stress and the vector of the mass transport according to (13) is represented in Fig. 2. It depends considerably on latitude, and reaches from 0° at the equator to about 90° at the poles. In the geostrophic case the angle is constantly 90°. Crossing the equator it jumps from 90° to -90°. At small friction, $r < 10^{-5}$ sec^{-1}, the angle increases from 0° at the equator rapidly to high values, in 20° latitude it has already reached 80°. At higher friction the increase is more gradual, at the poles 90° will never be reached.

It is very difficult to calculate values of r, using equation (12) because observations of the transport must be compared with observations of the stress, and both are difficult to observe. Few determinations already made are reported in table 1.

The determination of the coefficient r is simpler, using equation (13), which gives the angle of deflection as a function of the latitude. The Dutch Climatic Atlases for the China Sea and the waters around Australia, showing the resulting winds for 1° squares superimposed by the distribution of pressure, are especially suitable for this purpose. This allows an easy reading of the angle between the direction of the wind and of the pressure gradient. From these results the curve I in Fig. 2, showing

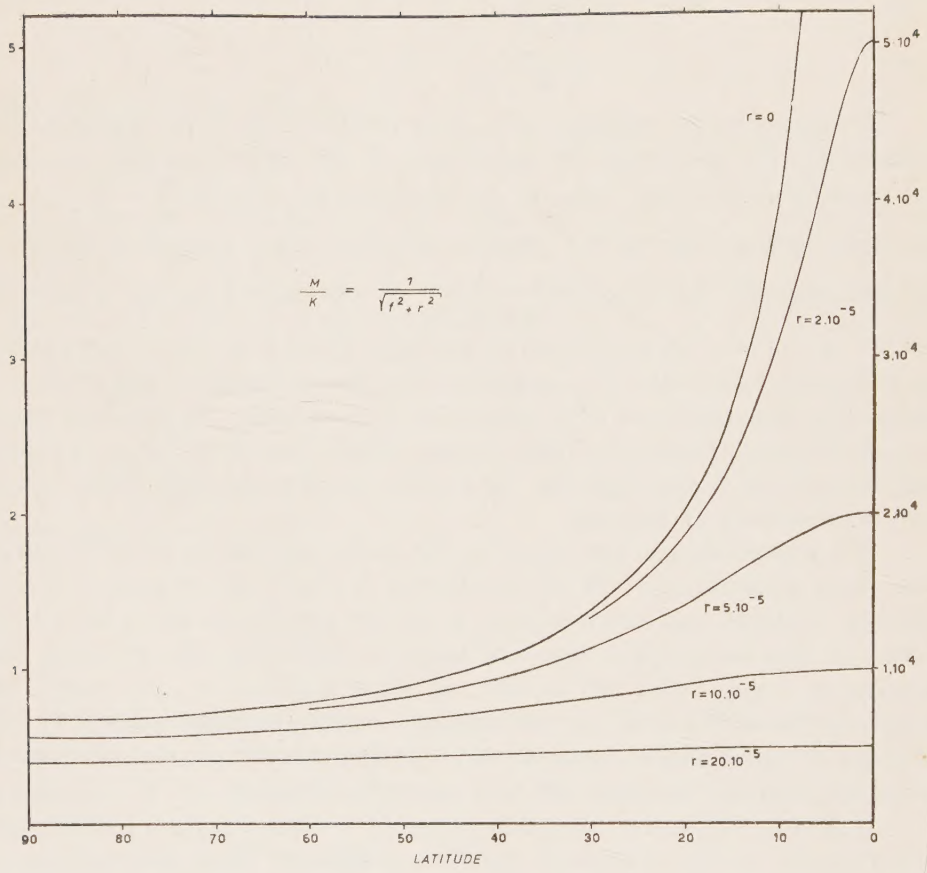

FIG. 1. Factor between mass transport and stress as a function of latitude for different friction coefficients.

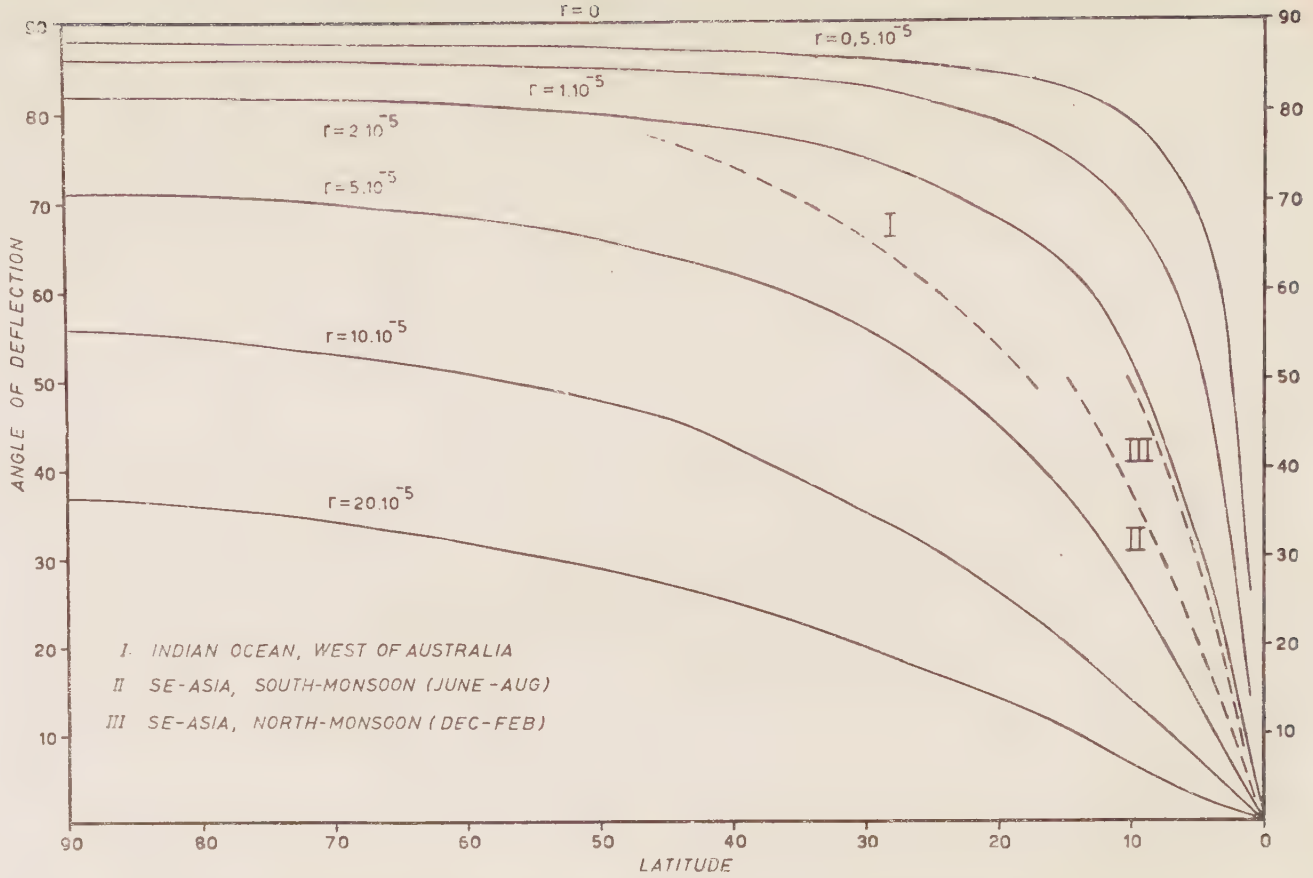

FIG. 2. Angle of deflection between the vector of mass transport and the vector of stress as a function of latitude for different friction coefficients.

this correlation between 15° and 50° S in the Indian Ocean west of Australia. For the Southeast Asian waters between 20°N and 20°S the curve II has been obtained for the south monsoon (July-September) and the curve III for the north monsoon (December-February). The north monsoon has a smaller friction then the south monsoon, for which a reason is difficult to give. The friction lies in all three cases between 2 and 4 10^{-5} sec^{-1}, and the curves run in fair agreement with the theoretical results. In an older publication SVERDRUP and HOLTSMARK (1917) have determinated these values over the United States and found r between 7 and 27 10^{-5} sec^{-1}, values which are essentially higher. But our values are found over the sea, where a smaller friction is expected. In table 1 the values of r are given which were known to the author to have been determinated, arranged separately for oceanic and meteorological conditions. It can be seen that higher values are found in waters where the currents reach towards the bottom than in waters of the open ocean. The reason is the friction at the bottom, as already discussed, when introducing the friction coefficient, equation (5). On the other hand, a relation between the coefficient r and the depth of the layer D seems to exist.

One could try to introduce another friction coefficient, the product r . D, in the hope that it might be independent of the special conditions. This coefficient has already been used by STOMMEL (1948) in his first publication on this subject. It seems unsatisfactory, however, because in this case it must also be considered that the friction depends on whether or not the velocity gradient vanishes in the depth D. The friction coefficient r varies from 0,3 10^{-5} in the open ocean to about 6 10^{-5} sec^{-1} in shallow waters. The high coefficients determinated experimentally by HANSEN (1951) are for depths below 10 m and velocities above 100 cm/sec.

Other assumptions have been made for the friction, especially as related to stresses. PROUDMAN (1953) makes very general use of the friction R in the form

$$R = \frac{1}{\varrho} \frac{\partial F}{\partial z} \tag{14}$$

where the stress F (dyne/cm^2) is given by

$$F = \varrho \, k \, u^2$$

and the constant k practically evaluates the friction. For R follows

$$R = k \, u \frac{\partial u}{\partial z}$$

and the friction R depends on the velocity as well as on the velocity gradient. A comparison with the coefficient of linear friction, defined by the relation

$$R = r \, u$$

TABLE 1. VALUES OF THE FRICTION COEFFICIENTS r AND k.

Region	r 10^{-5} sec^{-1}	D m	r D cm/sec	v cm/sec	k 10^{-3}	Calculated from	references and remarks
Pacific Ocean	0,1	200	0,02	10	2,0	estimated	STOMMEL (1948)
Atlantic Ocean	0,6	200	0,12	10	(12,0)	mass transport	HANSEN (1951) r = 2,0 found too high
Atlantic Ocean	0,33	300	0,1	10	(10,0)	deflection of surface drift	NEUMANN (1954)
Shallow waters	0,4-40	150-10	0,04-0,4	25-150	1,6-2,7	experimental and theoretical	HANSEN (1951)
Fehmarnbelt	2,0-4,0	30	0,06-0,12	50	1,2-2,4	wind, slope, currents	WYRTKI (1953/54)
Equatorial Pacific Ocean	0,5	100	0,05	25	2,0	wind, slope, currents	s. page 21
Java Sea	0,8	30	0,024	25	1,0	wind, slope, currents	s. page 24
North America over land	7-27					pressure, winds	SVERDRUP (1917)
Indian Ocean	2-4					angle of deflection between wind and pressure gradient	s. page 9
Southeast Asia	2-4					wind and pressure gradient	s. page 10, 18
Bristol Channal	1,2-3,2	50	0,06-0,16	40	1,4-4,1	slope, tidal currents	GRACE, (1936)
Strait of Dover	4,0-11,0	30	0,12-0,32	50	2,4-(6,3)	slope, tidal currents	GRACE, (1936)
Strait of Dover	6,0	30	0,19	50	3,8	wind, slope, currents	BOWDEN (1956)
North Sea	4,0-5,0	50	0,2-0,25	100	2,0-2,5	sterm surges	ALLARD (1952)
North Sea	3,0	50	0,15	50	3,0	estimated	HANSEN (1951)
Waters around The British islands	2,5	50	0,125	50	2,5	various methods, tidal currents	PROUDMAN (1953)

gives

$$r = k \frac{\partial u}{\partial z}.$$

Another approach leads to a better physical explanation of the meaning of the friction coefficient r. In the case, that all forces suddenly vanish, the equation of motion is

$$\frac{d u}{d t} = -R = -r u$$

By multiplying with ϱ u follows, because $\frac{1}{2} \varrho u^2 = E$ is the kinetic energy

$$\frac{d E}{d t} = -2 r E$$

This means that the friction coefficient r rules the time rate of the dissipation of the kinetic energy, which would be a physically convenient assumption for the friction.

On the other hand, the use of the friction according to equation (14) would give

$$\frac{d u}{d t} = \frac{1}{\varrho} \frac{\partial F}{\partial z}$$

and after the same operation

$$\frac{d E}{d t} = -4 k \frac{\partial u}{\partial z} E$$

In this case, the rate of dissipation would be a function of the velocity gradient, and would go to the limit zero in the same way as the energy.

For a comparison of the values of r and k, the velocity gradient will be replaced by the quotient of the average velocity $\bar{u}$ and the depth D of the motion,

$$r = \frac{k \bar{u}}{D}$$

The values of $\bar{u}$ and D have been estimated from the information given by the authors calculating values of k. In table 1 all the values of r calculated in this way are given.

It is remarkable that the coefficient k until now has been determinated only for tidal currents, where it has values between 1,5 and 4,0 10^{-3}, and 2,5 10^{-3} seems to be a relatively universal value, as shown by PROUDMAN (1953). The corresponding values of r range between 2,5 and 6,0-10^{-5} sec $^{-1}$. Interesting too are the values of k, derived from the values found for r. These vary between 1,2 and 2,7-10^{-3}, in fair agreement with the direct determinated values, except for the Atlantic Ocean, where both values are essentially higher. Generally it can be said that r is more variable then k, but with the restriction that k is determinated only for tidal currents.

TABLE 2. NUMERICAL VALUES OF THE FACTORS APPEARING IN EQUATIONS (8) AND (11) AS A FUNCTION OF THE GEOGRAPHICAL LATITUDE, FOR THE BOTH FRICTION COEFFICIENTS $r = 2\ 10^{-5}$ SEC^{-1} AND $r = 0{,}5\ 10^{-5}$ SEC^{-1}

φ	y	$\sin\varphi$	$\frac{f}{2\omega\sin\varphi}$	$r = 2\ 10^{-5}$		$\frac{1}{f}$	$r = 0{,}5\ 10^{-5}$	
				$\frac{r}{f^2+r^2}$	$\frac{f}{f^2+r^2}$		$\frac{f}{f^2+r^2}$	$\frac{r}{f^2+r^2}$
0	0	0.0	0.0	0.50	0.0	∞	0.0	2.0
1	1.1	0.017	0.25	0.49	0.062	4.0	0.81	1.61
2	2.2	0.035	0.51	0.47	0.120	1.96	1.00	0.98
3	3.3	0.052	0.76	0.44	0.166	1.32	0.92	0.60
4	4.4	0.070	1.02	0.40	0.202	0.98	0.79	0.39
5	5.6	0.087	1.28	0.35	0.227	0.78	0.68	0.264
6	6.7	0.105	1.53	0.32	0.241	0.65	0.59	0.193
7	7.8	0.122	1.78	0.28	0.248	0.56	0.52	0.146
8	8.9	0.139	2.03	0.25	0.250	0.49	0.47	0.116
9	10.0	0.156	2.28	0.22	0.248	0.44	0.42	0.092
10	11.1	0.174	2.54	0.191	0.243	0.39	0.38	0.075
11	12.2	0.191	2.79	0.170	0.237	0.36	0.35	0.062
12	13.3	0.208	3.04	0.151	0.229	0.33	0.32	0.053
13	14.4	0.225	3.29	0.135	0.221	0.304	0.30	0.045
14	15.6	0.242	3.53	0.122	0.215	0.283	0.28	0.039
15	16.7	0.259	3.78	0.109	0.207	0.264	0.26	0.034
16	17.8	0.276	4.03	0.099	0.198	0.248		0.030
17	18.9	0.292	4.26	0.090	0.192	0.234		0.027
18	20.0	0.309	4.51	0.082	0.186	0.222	$= \frac{1}{f}$	0.024
19	21.1	0.326	4.76	0.075	0.179	0.210		0.022
20	22.2	0.342	5.00	0.069	0.172	0.200		0.020
21	23.3	0.358	5.22	0.064	0.167	0.192		0.018
22	24.4	0.375	5.46	0.059	0.161	0.183		0.017
23	25.6	0.391	5.70	0.055	0.156	0.175		0.015
24	26.7	0.407	5.94	0.051	0.151	0.168		0.014
25	27.8	0.423	6.16	0.048	0.147	0.162		0.013
	10^7 cm		10^{-5} sec^{-1}	10^5 sec	10^5 sec	10^5 sec	10^5 sec	10^5 sec

When using friction in oceanographic computations, it must be first determined which special assumptions will be made on it. Sometimes the mathematical point of view might prefer a special assumption, because in the other case the mathematical effort would become too voluminous. For the physical point of view, it might be preferable to use the assumption

$$R = k u \frac{\partial u}{\partial z}$$

with the coefficient k, in cases where the vertical velocity gradients play an important role, for instance in tidal currents over shallow water, and the assumption

$$R = r u$$

with the coefficient r, in the open ocean.

In order to get an impression, and for the use in calculations, both factors

$$\frac{r}{f^2 + r^2} \qquad \text{and} \qquad \frac{f}{f^2 + r^2}$$

appearing in equation (8) and (11) have been tabulated together with $f = 2\omega \sin \varphi$ and 1 f in table 2, for the equatorial belt between 25°N and 25°S and for two friction coefficients $r = 2\ 10^{-5}$ sec^{-1}, which is approximately valid in coastal waters, and $r = 0{,}5\ 10^{-5}$ sec^{-1}, which is met in the ocean.

Moreover, it is remarkable that the friction coefficients for the ocean and the atmosphere are approximately the same, which means that the dissipation of energy takes place in about the same way.

Models of atmospheric circulation. To study the properties of simple fields of motion resulting from the application of the linear friction coefficient, some typical cases of circulation across the equator are presented, because there geostropic winds can not be computed, and the effects of the consideration of the friction appear most clearly. The basis is the equation (9) and a friction coefficient $r = 2\ 10^{-5}$ sec^{-1}, In 8° latitude it is $r = f = 2\omega \sin 8°$.

The first example (Fig. 3) shows the wind distribution computed from isobars parallel to the equator, the high in the north, the low in the south, according to the north monsoon over South East Asia. The isobars are equidistant, which leads to maximal velocities at the equator. This condition is not met normally, as will be shown later. At the equator the direction of the wind is exactly to the south. With increasing latitude it changes rapidly to a more geostrophic direction.

In Fig. 4, the equidistant isobars cross the equator at an angle of 45°, the high lying in the southeast and the low in the northwest. The

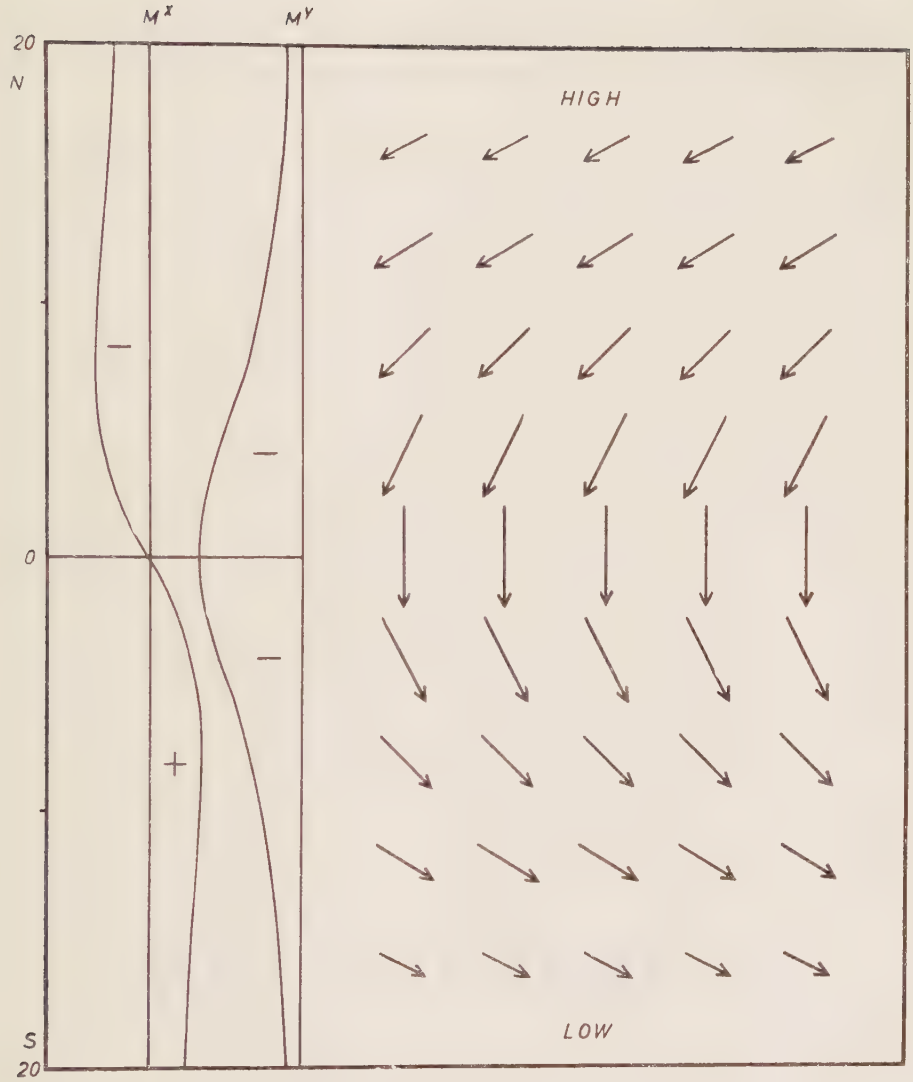

FIG. 3. Velocity distribution in the vicinity of the equator for equidistant isobars parallel to the equator.

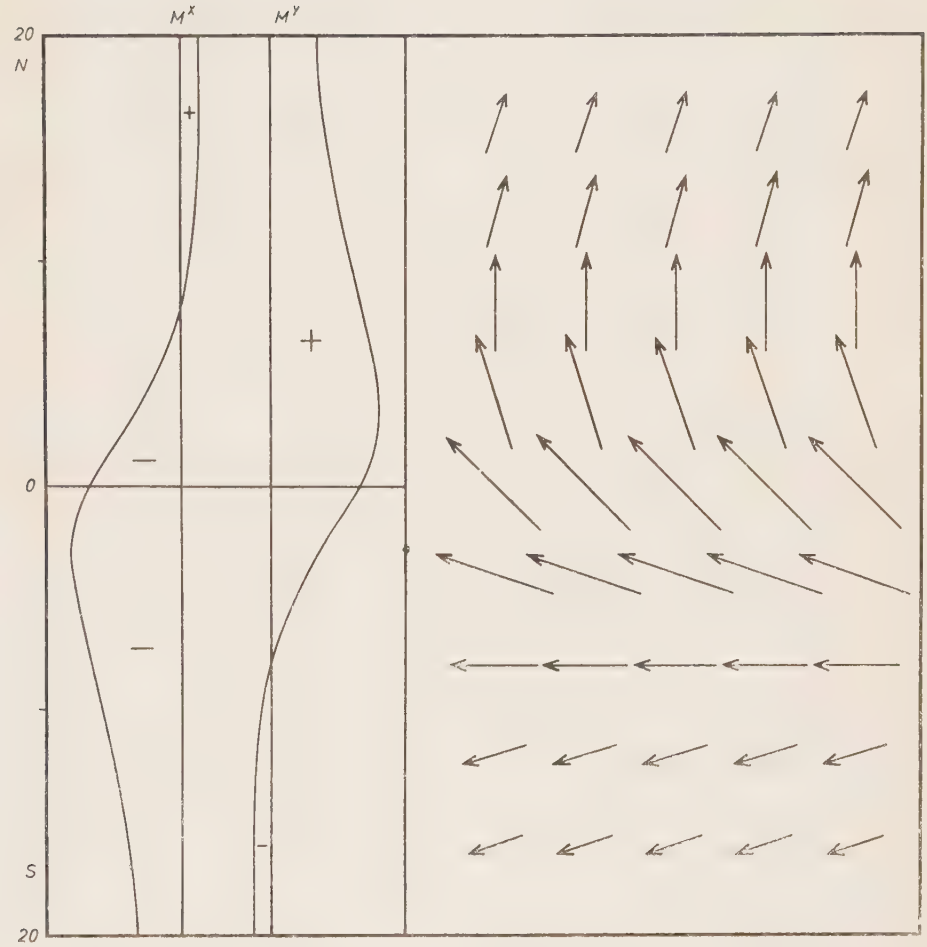

FIG. 4. Velocity distribution in the vicinity of the equator for equidistant isobars crossing the equator under 45°.

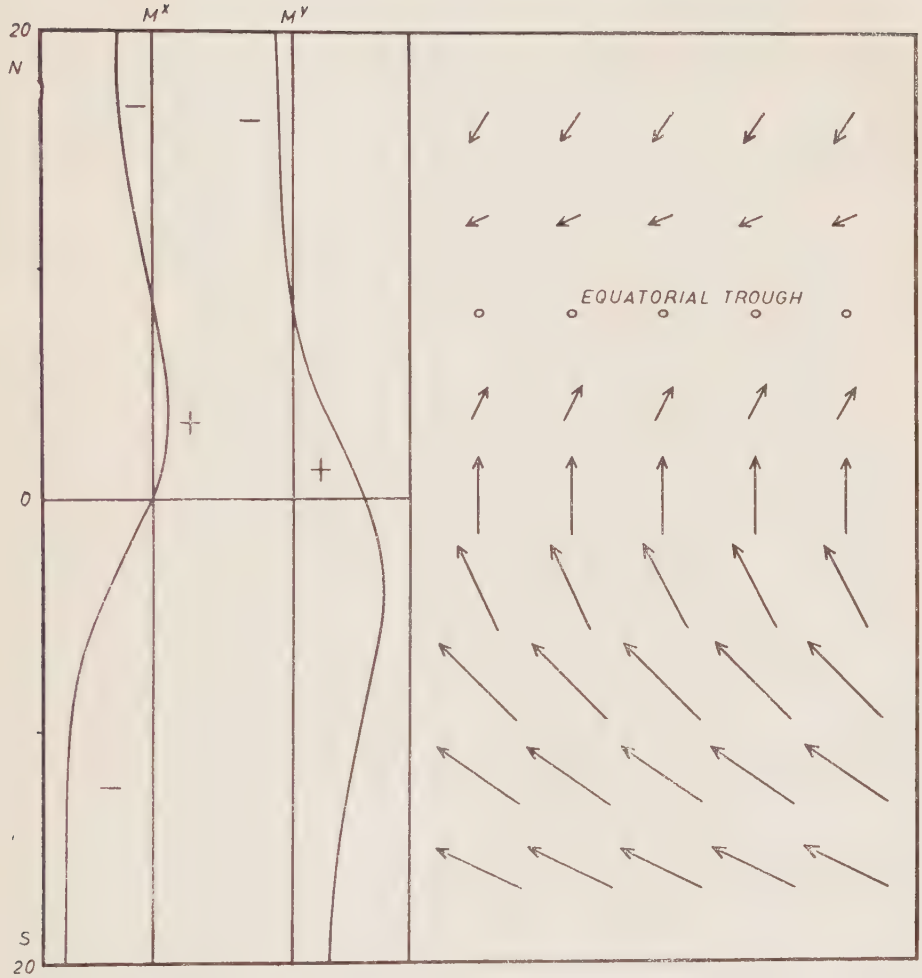

FIG. 5. Velocity distribution in the vicinity of the equator for a pressure trough at 8° North.

wind field also shows a typical monsoon character. In contrast to the observations, the maximal velocities are at the equator. In fact, the distribution of pressure will adjust in such a way that the distribution of wind becomes equalized.

The distribution of winds at both sides of a pressure trough situated at 8°N, asymetrically to the equator, is shown in Fig. 5. The pressure is given by $p = p_0 - p_1 (y - a)^2$. Such a distribution might be found in rough approximation off the west coast of Central America in August. A comparison with the wind charts given by SCHOTT (1935), shows that the winds are strongest just south of the equator, pass the equator in a northerly direction, and have a small west component north of the equator. North of the doldrums, weak north east winds are found. All this is in agreement with the distribution shown in Fig. 5.

Two more realistic distributions are shown in Figs. 6 and 7. The distribution of pressure has been obtained between Hong Kong and Pt. Shedland in northwest Australia for January and August from the Dutch Climatological Atlases. The isobars, in first approximation, can be considered to be parallel to the equator, so that the pressure and the components of the velocity depend only on y. This is not completely true in the region south of 15°S in January and north of 15°N in August. Both representations show that the pressure gradients have a minimum in the vicinity of the equator, but they do not vanish. The velocities have been computed with a friction coefficient $r = 2\ 10^{-5}\ sec^{-1}$, and show a minimum of velocity at the equator. In agreement with the observations the maximal velocity is reached in both cases over the China Sea and over the Indian Ocean south of Java. During the north monsoon in January, especially over the China Sea, high velocities are found, often exceeding Beaufort 6. The south component of the velocity is relatively constant during the north monsoon, while during the south monsoon in August, it has a maximum at the equator. The angle of deflection (Fig. 7) increases from 0° at the equator rapidly to 45° in 8° latitude and exceeds 60° in 15° latitude. In 20° the deviation from the geostrophic direction is weak. The calculated velocities and their distribution are in fair agreement with the observations shown in both atlases.

Application to the equatorial currents in the Pacific Ocean. The region in which the method can be most effectively proved is the vicinity of the equator, and therefor an attempt to calculate the distribution of velocity in the Central Pacific from the distribution of wind and pressure has been made. The conditions represented in Fig. 8 are approximately

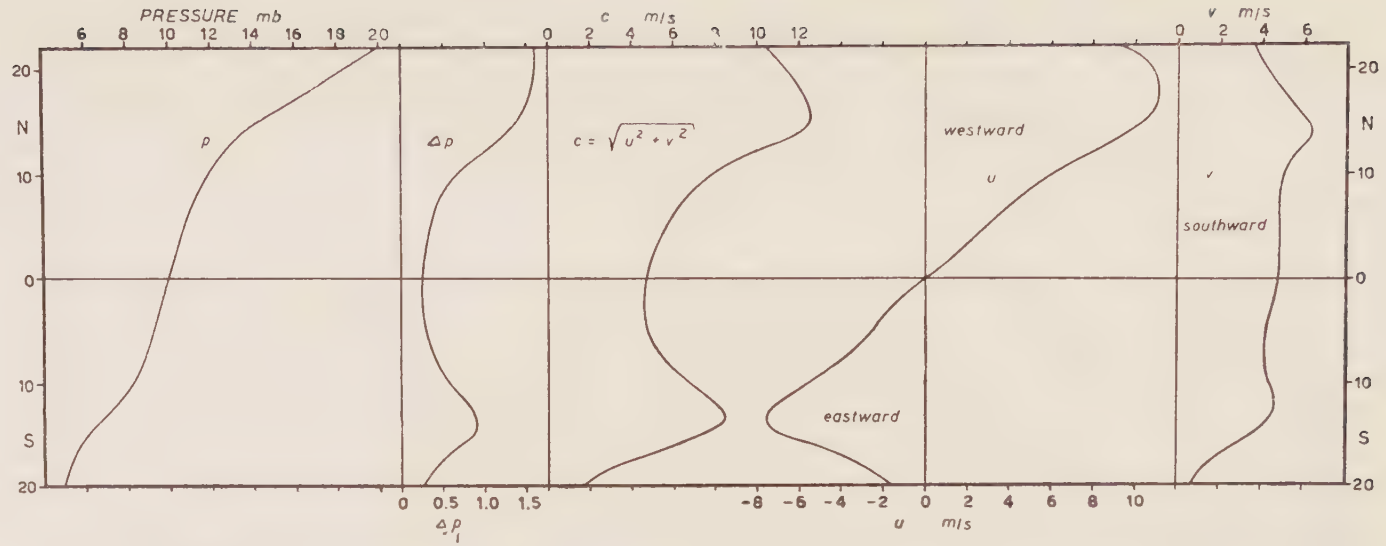

FIG. 6. Distribution of pressure along a section from Hong Kong to Pt. Hedland, Australia, during the north monsoon in January, with derived wind velocity distribution.

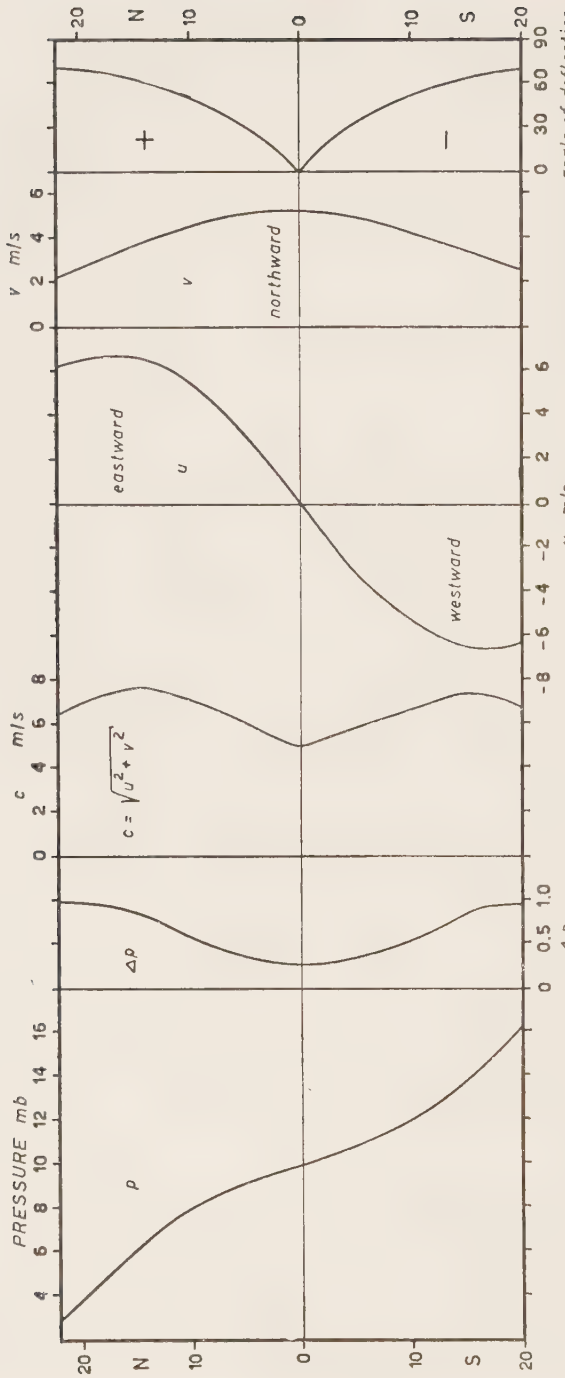

FIG. 7. Distribution of pressure along a section from Hong Kong to Pt. Hedland, Australia, during the south monsoon in August with the derived wind velocity distribution.

these at 160°W, between 20°N and 10°S, in September/October, when the Equatorial Counter Current is strongly developed. The components of the wind stress show the northeast Trades with a component in a southerly direction, show the doldrums in 8°N, and show the southeast Trades with a component in a northerly direction reaching its strongest developement just south of the equator. The topography of the sea level has been taken from the Carnegie observations, given by SVERDRUP (1945) relative to the 2000 decibar level.

In Fig. 8 the sea level, as well as the slope h_y, is presented. The longitudinal slope is computed to be $h_x = 0{,}45\ 10^{-7}$, according to an increase of the surface of 60 cm within 120° of longitude. It is considered to be independent of latitude, because this factor gives only a small contribution to the calculated values.

With these assumptions the components of the mass transport M^x M^y have been computed from equation (8), with a friction coefficient $r = 0{,}5\ 10^{-5}$ sec^{-1}. Relating these transports to a layer of 100 m, in which the density is assumed to be constant so that the distribution of pressure might not change essentially, one obtains the components of the velocity u and v, shown in Fig. 8. Simultaneously, the equation of continuity gives the vertical movements in the depth D, which is 100 m, showing the regions of descending and ascending motion which are, respectively, the convergences and divergences at the surface.

The results show the Counter Current between 4° and 10°N clearly, with maximal velocities above 50 cm/sec, and show also a southern component at the surface. The North Equatorial Current is relatively weak and reaches velocities of only 14 cm/sec, while the South Equatorial Current exceeds 25 cm/sec. Its maximal velocities are on both sides of the equator, and at the equator a belt of reduced velocities is found. This belt might be the Equatorial Undercurrent, which has been discovered by CROMWELL, MONTGOMERY and STROUP (1954), and has been explained theoretically by FOFONOFF and MONTGOMERY (1955). The belt of reduced velocities extends to about 1,5 degrees on both sides of the equator. Because the velocities calculated here are averages between the surface and 100 m, there will be no reverse flow indicated. The maximum of the velocity of the Equatorial Undercurrent is found at the upper limit of the discontinuity layer in about 100 m depth. It is surprising that such a detail of the circulation can be found, even using such simple methods.

A remarkable supplement to this picture is given by the meridional components of the velocity and by the vertical components in 100 m. The Counter Current has a distinct component to the south, while the North

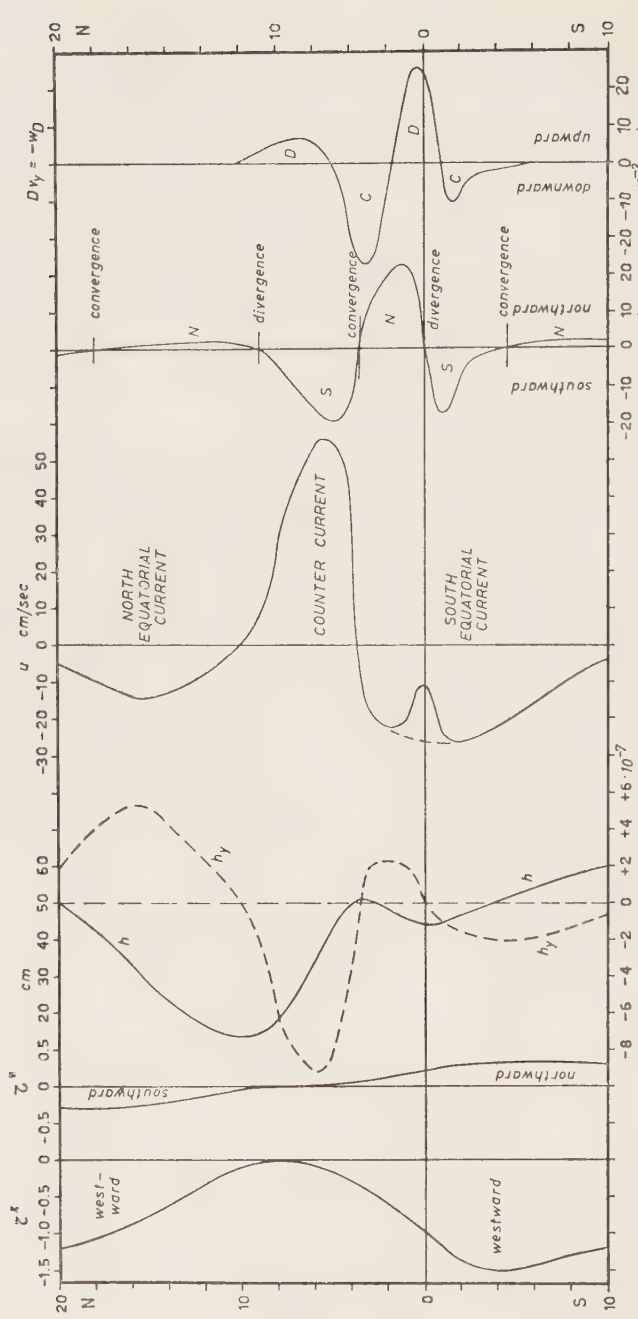

FIG. 8. Wind stress components and topography of the sea level along a section across the equator at about 160°W with derived velocity distribution in the layer between the surface and 100 m depth, and vertical movements at 100 m.

Equatorial Current has a weak northerly component, producing at their boundary a divergence. This is characterised also in the vertical motion in 100 m, and reaches from about 5° to 11°N with ascending motion. At the boundary between the Counter Current and the South Equatorial Current a convergence is formed with descending movements in the depth. Interesting is the solution at the equator itself. The movements are northward north of the equator and southward south of the equator, producing a divergence at the equator and ascending motions in the depth. In about 2°S, again a region of descending motion is found in connection with a convergence at the surface at about 5°S. This picture of the movements is in fair agreement with that derived by SVERDRUP (1946, p. 710) from the distribution of different properties along a section crossing the equator. These calculations, however, do not allow arriving at conclusions on the reason of the pressure distribution. Observed wind stresses and the pressure distribution are required in this method, from which the distribution of movements can be computed. On the other hand, SVERDRUP (1947) has shown that it is possible to compute the distribution of pressure or, identically, the topography of the sea level, from the distribution of wind stress. With this he has demonstrated that the whole current system near the equator is an effect of the wind distribution. The computation of motion by means of the observed pressure and wind distribution used in this paper, however, gives more detail of the motion, and especially of the vertical movements, which are of importance for the explanation of various effects. Therefore, this treatment is especially suitable for the interpretation of oceanographic observations in only parts of the oceans.

Application of the method for channels. Channels or other passages often allow very simple applications of the equation (7). It is reasonable to assume that the mass transport across the channel vanishes, at least its integral from one boundary to the other. Putting the coordinate system in such a way that the x-axis points in the direction of the channel, and integrating over the width b of the channel, one obtains

$$\int_0^b M^y \, dy = 0 \qquad \text{and} \qquad \int_0^b M^x \, dy = T$$

where T is the transport in g/sec. With the assumption that the wind stress τ is independent of y, the first both equations of (7) are

$$\begin{aligned} r\,T &= b\,\tau^x - \varrho\, g\, D\, b\, h_x \\ f\,T &= b\,\tau^y - \varrho\, g\, D\,(h_b - h_o) \end{aligned} \tag{15}$$

where $h_b - h_o$ is the difference of the sea level between both shores. Considering at first a wind blowing parallel to the channal, $\tau^y = 0$, as it is during the monsoons over the Java and China Seas, and of a vanishing slope in the direction of the channal, $h_x = 0$, which is fixed by observations, the system (15) is reduced to

$$r\,T = b\,\tau^x$$
$$f\,T = -\varrho\,g\,D\,(h_b - h_o)$$

These equations allow the elimination of two factors, for instance of the friction r and of the transport T, if the windstress τ and the sea level difference $(h_b - h_o)$ are known, as well as the dimensions of the channel. For the Java Sea during the south east monsoon these are approximately

$$\tau^x = -0{,}8 \text{ dyne/cm}^2,\ b = 3\ 10^7 \text{ cm},\ D = 30\ 10^2 \text{ cm},$$
$$f = 2\,\omega \sin 5^\circ = 1{,}2\ 10^{-5} \text{ sec}^{-1},\ (h_b - h_o) = 12 \text{ cm}$$

with the solution

$$T = -3\ 10^{12} \text{ g/sec} \sim 3 \text{ million m}^3\text{/sec}$$
$$r = 0{,}8\ 10^{-5} \text{ sec}^{-1}$$

The average velocity over the whole section is computed from $v\,b\,D = T$ and gives 33 cm/sec, which is in agreement with the observations. The friction r is larger than in the open ocean, but lower than in the narrower channel of the Fehmarn-Belt, see table 1. Carrying out the computation in this way, the cross slope seems to be the ruling factor. Actually, the transport is produced by the wind stress with the friction as limiting factor. But because of the coriolis acceleration, there is a component vertical to the wind, which must be balanced by a cross slope, which is maintained by that wind.

In the southern part of the China Sea, just below the equator, the conditions are rather different. Here is $f = 0$, and the wind is in the direction of the channel. It follows from equations (15) that

$$r\,T = b\,\tau^x,$$

while the left side of the second equation vanishes. A cross slope can be produced only by a west - east component of the wind, and does not affect the transport

$$b\,\tau^y = \varrho\,g\,D\,(h_b - h_o).$$

Because, in this case, only one equation is available, it is impossible to determinate r and T. But we must assume that the transport through the southern China Sea is equal to the transport through the Java Sea at the same time. Therefore it is

$$T = 3\ 10^{12} \text{ g/sec} \quad b = 4\ 10^7 \text{ cm} \quad \tau^x = 0{,}6 \text{ . dyne/cm}^2$$

and with it

$$r = 0{,}8\ 10^{-5} \text{ sec}^{-1},$$

which is the same friction as in the Java Sea. If such a transport should be maintained by a longitudinal slope, it would have to be

$$r\,T = -\varrho\,g\,D\,b\,h_x$$

and with the values used above

$$h_x = 3\ 10^{-7}$$

But a stationary slope of $3\ 10^{-7}$, which is 15 cm within 5° of latitude, does not appear in these waters in the direction of the current. This might appear only in tidal currents, where the slope is not stationary.

In the China Sea the conditions during the south west monsoon are rather different. The wind stress $\tau^x = 0{,}9$ would produce a transport of $T = 8\ 10^{12}$ g/sec, using a width of the channel b = 700 km, and a friction $r = 0{,}8\ 10^{-5}$ sec^{-1}. But such a transport does not appear, because only $3\ 10^{12}$ g sec of water will be delivered from the Java Sea. Therefore, a part of the wind stress must be compensated by a longitudinal slope of the sea level against the current. Using the first equation of (15) with D = 80 m, and a slope of 16 cm on 20 degrees of latitude, according to observations, it is

$$r\,T = b\,(\tau^x - \varrho\,g\,D\,h_x)$$

and with $T = 3\ 10^{12}$ g/sec follows a friction $r = 0{,}6\ 10^{-5}$ sec^{-1}.

This friction is smaller than in the Java Sea, because the currents do not touch the bottom in the largest parts of the region. From the second equation of (15), the cross slope can be calculated to be 11 cm over the full width of the channel, if there is no wind component across the channel. This is in agreement with the observations too. The velocity can be computed from the transport, the width of the channel and the depth of the current, to average 4,2 cm/sec between the surface and 80 m. Because the velocity vanishes at 80 m, it will be about 10 cm/sec at the surface, which agrees closely with the observations.

References

Allard, P., 1952. C. O. E. C. Bull. Inform. 4, 307.

Bowden, K. F., 1956. The flow of water through the Strait of Dover. Phil. Trans. Roy. Soc. Lond. No. 953, Vol. 248.

Cromwell, T., Montgomery, R. B. and Stroup, E. D., 1954. Equatorial Undercurrent in Pacific Ocean revealed by new methods, Science, 119.

Defant, A., 1941. Die absolute Topographie des physikalischen Meeres niveaus und der Druckflächen sowie die Wasserbewegungen im Raum des Atlantischen Oceans. Meteor-Expedition, Vol. 6, Teil 2,5.

Fofonoff, N. P. and Montgomery, R. B., 1955. The Equatorial Undercurrent in the light of the Vorticity Equation. Tellus, 7,4.

Grace, S. F., 1936. Friction in the tidal currents of the English Channel. Geophys. Suppl. M. N. R. Astr. Soc. Vol. 4, p. 133.

Hansen, W., 1951. Beobachtungen des Windstaus und Triftstroms im Modellkanal. Dtsch. Hydr. Z. Bd. 4, Heft 3.

Hansen, W., 1951. Winderzeugte Strömungen im Ozean Dtsch. Hydr. Z. Bd. 4, Heft 4.

Hansen, W., 1952. Dtsch. Hydr. Z. Ergänzungsheft 1.

Hidaka, K., 1950. Lateral mixing and wind driven currents in an enclosed ocean. Journ. Mar. Res. Vol. 9, p. 55.

Hidaka, K., 1955. A theoretical Study on the general circulation of the Pacific Ocean. Pacific Science, Vol. 9, p. 183.

Hidaka, K., 1955. Divergence of surface drift currents in terms of wind stresses. Jap. Journ. of Geophy. Vol. 1, No. 2.

Munk, W. H., 1950. On the wind driven ocean circulation. Journ. Meteorology. Vol. 7, No. 2.

Neumann, G., 1954. Notes on the wind driven ocean circulation. New York Univ., Dept. of Meteor. and Ocean.

Proudman, J., 1953. Dynamical Oceanography, London, 1953.

Rossby, C. C., 1936. Dynamics of steady ocean currents in the light of experimental fluid mechanics. Pap. Phys. Ocean. Meteor. 5, 1.

Schott, G., Geographie des Indischen und Stillen Oceans, Hamburg, 1935.

Stommel, H., 1948. The westward intensification of wind driven ocean currents. Trans. Amer. Geophy. Union, 29, 2.

Sverdrup, H. U. and J. Holtsmark, 1917. Veröff. Goephy. Inst. Leipzig, 2, 2, 97.

Sverdrop, H. U. a.o. 1945. Carnegie Expedition, Oceanography, I B.

Sverdrup, H. U. a.o. 1946. The Oceans, New York 1946.

Sverdrup, H. U. a.o. 1947. Wind driven currents in a baroclinic ocean. Proc. Nat. Acad. Sci. 33, p. 318.

Wüst, G., 1950. Blockdiagramme der atlantischen Zirkulation. Kieler Meeresforsch. 7, 1.

Wyrtki, K., 1953, 1954. Die Dynamik der Wasserbewegungen im Fehmarnbelt, Kieler Meeresforsch. 9,2 u. 10,2.

Sea areas round Australia, Koninklijk Nederlands Meteorol. Inst., No. 124.

Oceanographic and meteorological observations in the China Sea. Koninklijk Nederlands Meteorolog. Inst. No. 115, 1936.

SURFACE SALINITIES IN THE STRAIT OF MALACCA

by

Rd. E. Soeriaatmadja

Summary

A continuous northwest-going current prevails in the Strait of Malacca throughout the year, except June and August, when the currents are very weak and sometimes reversed in the southern part.

The southern part of the Strait of Malacca is influenced by the currents. These currents transport low saline water into the Strait during the southwest monsoon and high saline water from the South China Sea during the northeast monsoon.

In the northern part, the rainfall is of greater importance for the variations of the surface salinity and a strong correlation between rainfall and surface salinities is found in this region.

It is unlikely that Indian Ocean water penetrates the South China Sea.

Zusammenfassung

Eine ständige Strömung nach Nordwesten herrscht in der Malakka-Strasse während des ganzen Jahres mit Ausnahme der Monate Juni und August, in denen die Strömungen im südlichen Teil sehr schwach sind und zeitweilig entgegengesetzt verlaufen.

Der südliche Teil der Malakka-Strasse steht unter dem Einfluss dieser Strömungen. Sie transportieren während des Südwest-Monsuns salzarmes Wasser in die Strasse und während des Nordost-Monsuns salzreicheres aus der südlichen China See.

Im nördlichen Teil ist der Niederschlag von grösserer Bedeutung für die Schwankungen des Salzgehaltes an der Oberfläche, und eine Korrelation zwischen dem Niederschlag und dem Salzgehalt ist in diesem Teil vorhanden.

Es ist unwahrscheinlich, dass Wasser aus dem Indischen Ozean in die Südliche China See gelangt.

Ichtisar

Arus kearah barat laut jang terus menerus berlangsung sepandjang tahun diselat Malaka, ketjuali dalam bulan Djuni dan Agustus, dalam waktu-mana arus itu sangat lemah dan kadang-kadang membalik dibagian selatan.

Bagian selatan selat Malaka dipengaruhi oleh arus. Arus ini memindahkan air jang berkadar garam rendah keselat itu selama musim barat daja dan air jang berkadar garam tinggi dari Laut Tiongkok Selatan selama musim timur laut.

Dibagian utara, turun hudjan adalah penting sekali bagi perubahan-perubahan kadar garam dipermukaan dan hubungan pengaruh-mempengaruhi jang kuat antara turun hudjan dan kadar garam dipermukaan terdapat dibagian ini.

Rupa-rupanja tidak mungkin, bahwa air lautan Hindia meresap ke-Laut Tiongkok Selatan.

As is known, the production of fish depends mainly on the availability of food which, in turn, depends on the production of phytoplankton, because the latter forms the basic product in the cycle of organic matter. Physical and chemical factors which favour this production are to be found in the Strait of Malacca. The energy for the photosythetic process is sufficient as everywhere in tropical waters. The nutrient salts, phosphates and nitrates, which form a limiting factor in the phytoplankton production, seem to be sufficient too, because the Strait has influx of considerable fresh water containing nutrients from the land. The southern part of the Strait of Malacca is shallow, so that the sinking detritus containing organic matter which is regenerated at the bottom, could be distributed again into the whole water column by vertical mixing. According to K. M. WEEL's observations (1923), there is a great difference in salinity between the bottom layers and surface layers in the nothern section of the Strait throughout the year, except for a few weeks during or about August, wherein the salinity of the surface layer is about the same as that of the bottom layer. The data concerning the currents in the Strait of Malacca, show a continuous northwest-going current throughout the year, except in June and August, during which the water movements are very weak and sometimes reversed in the southern part. North of One Fathom Bank (about lat. 3° N.), the transport of less saline water in a northwesterly direction causes an opposite current in the deeper layers. This bottom current ascends when reaching the slope of the One Fathom Bank, and passes over into the surface current. This means that the nutrients from the bottom are distributed again into the whole water column.

These are the reasons that the Strait of Malacca is assumed to have a high potential production of fish.

The movements of watermasses with different salinities may be expected to play an important role on the migration of fish. For that reason, the author presents this paper, which could be used in fisheries hydrography.

The present paper is based on data of the years 1949-1954, consisting of 33.808 observations, which were collected for the Institute of Marine Research at Djakarta with the coöperation of Captains and Officers of several shipping companies, which operate regularly in the Strait of Malacca.

For the methods of collecting data, of analyzing samples, and of plotting them on the charts, the author refers to the previous papers of P. CH. VEEN (1951 and 1953) and E. SOERIAATMADJA (1956) as these

methods have remained exactly the same, so that a redescription is considered unnecessary here.

The area surveyed is the whole Strait of Malacca situated between Sumatra and the Malay peninsula, including its southern and northern entrances. The southern entrance is formed by the island group with several small passages South of Singapore, and the wide northern entrance is defined by a line connecting the north point of Sumatra with the island Lantar near the west coast of Malacca. The bottom of the Strait of Malacca shows a gradual slope from the coasts of East Sumatra and West Malacca to the centre of the Strait and can be divided into two parts by a threshold near the One Fathom Bank, from which place the bottom shows an increase in depth towards the Indian Ocean and towards the South China Sea. The increase towards the Indian Ocean is much greater than that towards the South China Sea.

The salinity data by months were averaged for each 20′-square, plotted on the chart, and the isohalines drawn with intervals of $0.5^0/_{00}$. The solid lines illustrate the even numbers, while the dotted lines the odd numbers of the salinities. Each chart is provided with an insert, on which the directions of the surface currents, according to the Atlas surface currents of the U.S. Navy Hydrographic Office, were drawn for the same month.

To gain a better insight into the annual variations of the surface salinities and their annual means, in the centre of the northern, middle and southern parts of the Strait of Malacca, Fig. 1 was prepared. The graphs are based on the average of the salinity values for each month. The solid lines represent the northern part between lats. 3° 40′ N. and 5° N., the dotted lines represent the middle part just north of One Fathom Bank, while the cross lines represent the southern part of the Strait of Malacca.

The salinity in the northern part shows two maxima and two minima. The maximum in August with a salinity of $32.0^0/_{00}$ is higher than that in February. The minimum in December with a salinity of $30.6^0/_{00}$ is lower than that in May. Compared with the salinity in the northern part, the salinity in the middle part shows a much lower value in all months. The maximum of $31.2^0/_{00}$ occurs in July, the minimum of $28.9^0/_{00}$ in December, corresponding with that in the northern part. A secondary minimum of $30.1^0/_{00}$ is to be noted in May, also corresponding with a minimum in the northern part. Compared with the first two graphs, that of the southern part shows a quite different picture. There is only one maximum of $30.8^0/_{00}$ occuring in March and one minimum of $28.3^0/_{00}$ occuring in October. Both extreme values occur earlier than in the middle

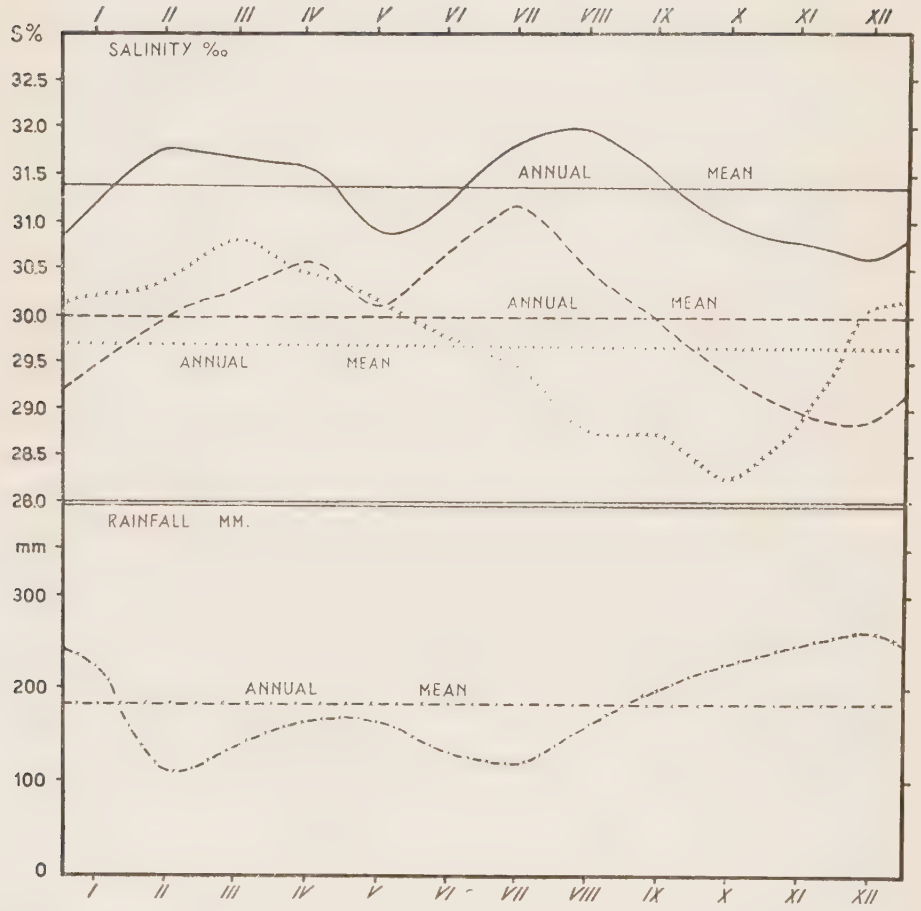

FIG. 1: Annual variations of the surface salinities and their annual means in the centre of the northern part (solid lines), the middle part (dotted lines), and the southern part (cross lines) of the Malacca Strait, and rainfall in the coastal region of the Strait of Malacca. Data from Verhandelingen No. 37, 1949.

part. Describing the salinity pattern in the Strait of Singapore, THAM AH KOW (1953) found in 1948-1949 two maxima, one during March-April, the other during November, and two minima, one during December-January, the other July-August. For the region off the bay of Djakarta in the Java Sea, the writer found, in the period 1949-1955 two maxima, one during May, the other during October-November, and two minima, one during January-February, the other during July, while for the region off the north coast of Madura there was only one maximum during September, and one minimum during April.

The annual range in salinity in the northern, middle and southern parts of the Strait of Malacca are 1.4‰, 2.3‰ and 2.5‰ respectively, while the absolute salinity minimum is 2.3‰ lower in the southern part than that in the northern part.

It is interesting to compare the salinity data of the northern part of the Malacca Strait with the data of rainfall in he coastal area of the Malacca Strait (Fig. 1). A strong correlation is noted between the rainfall and surface salinities in this region.

Figures 2 and 3 were prepared to gain a better insight into the surface salinity distributions in the Strait of Malacca. Fig. 3 represents isopleths of the surface salinity of the region investigated according to the line extending across the Strait from long. 97° E. and lat. 5° 40′ N. towards long. 105° 10′ E. and lat. 0° 30′ N. as shown in Fig. 2.

In studying the twelve charts and the figures, some remarkable facts are noted.

According to the Malacca Strait Pilot (1946), there is a current in a general northwesterly direction through the central part of the Strait throughout the year. As a consequence, the water from the Strait emerges into the Indian Ocean in a westerly or northwesterly direction. In the full southwest monsoon period of June-July, a current flows along the eastern part of the Andaman Sea along the west coast of the Malay peninsula southward, but turns to the west before entering the Strait of Malacca. This current meets the westgoing current, emerging from the Malacca Strait between about lats. 6° N., penetrating the Indian Ocean.

During the northeast monsoon period of October-April, a southgoing current prevails in the South China Sea, adducing water over 32.0‰ from the South China Sea through the Gaspar and Karimata Straits into the Java Sea. This southgoing current causes a branch, which rounds the Malay peninsula in the south, entering the Malacca Strait. The branch is demonstrated by an invasion of the South China Sea water into the Strait of Malacca, replacing the low saline water in the southern part of the Strait. The

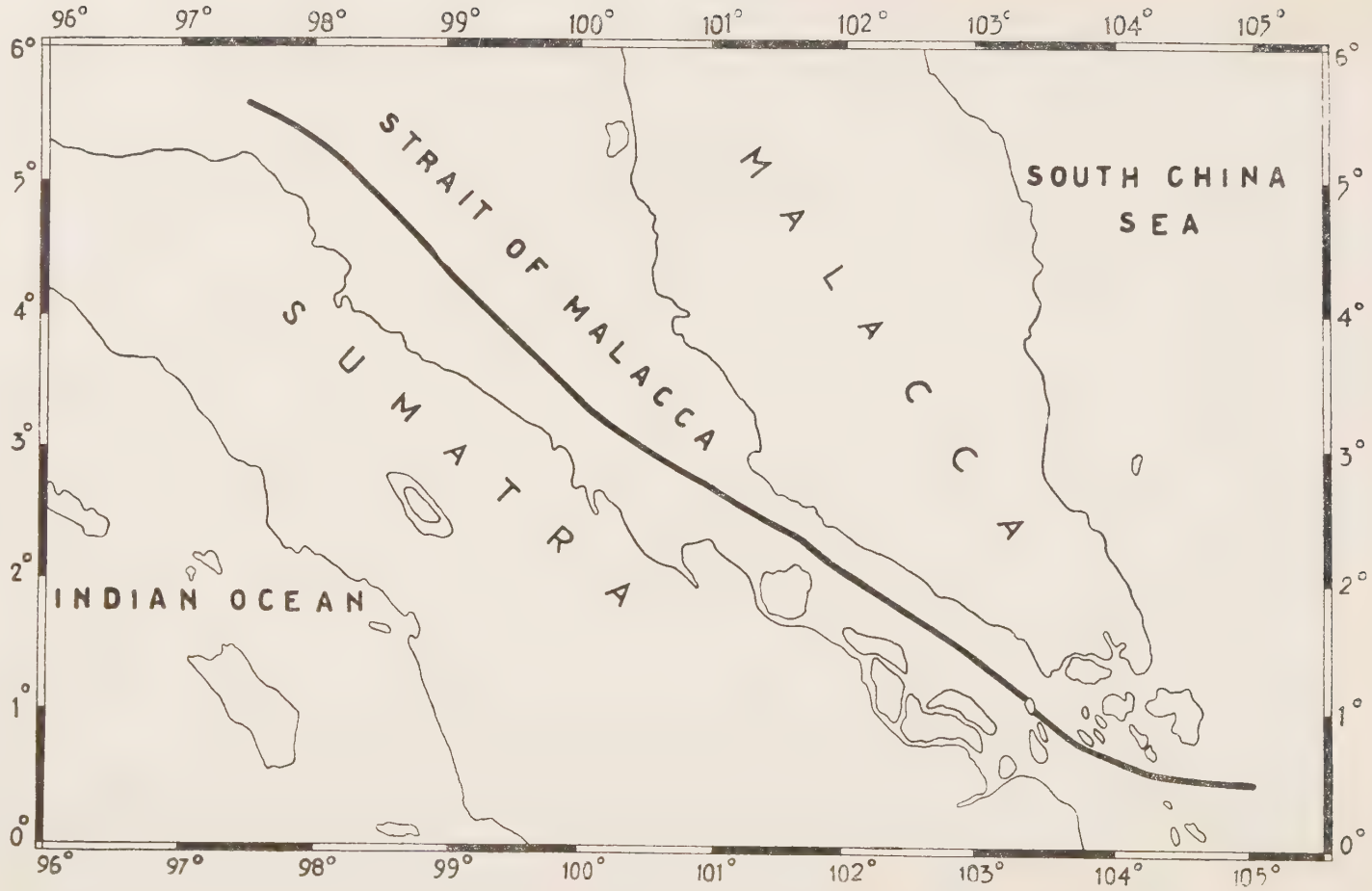

FIG. 2: Section through the Strait of Malacca along which the isopleths of Fig. 3 are drawn.

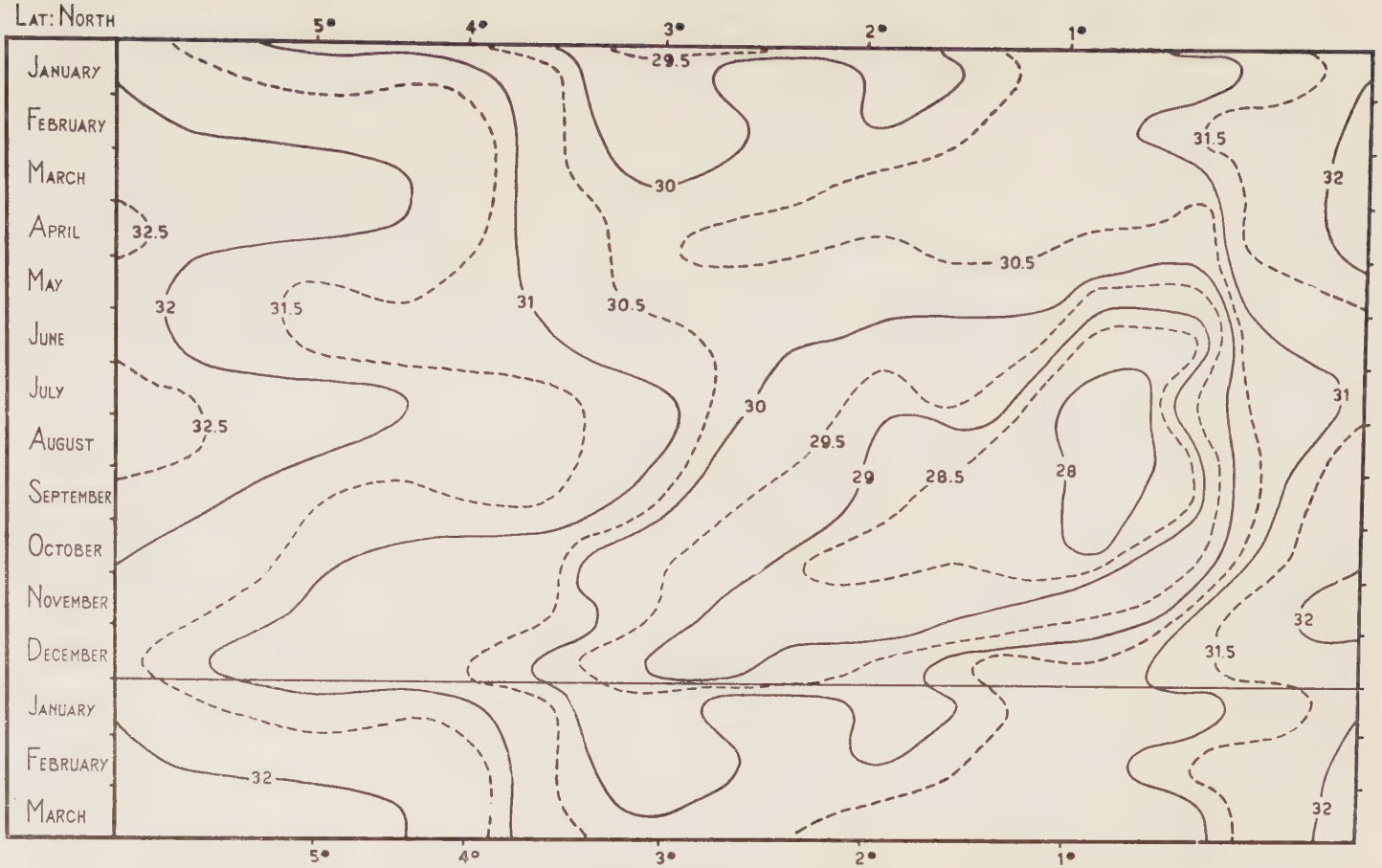

FIG. 3: Isopleths of surface salinity along the Strait of Malacca, as shown by the line in Fig. 2.

low saline water in the southern part moves slowly northward and mixes with the higher salinities in the northern part. The invasion of the higher saline water from the South China Sea into the Strait of Malacca is illustrated first by an increase in salinity in the southern part (after October) to its maximum in March, and second by a higher salinity in the southern part than that in the middle part during the period of December-March. In spite of heavy rainfall, an increase in salinity is maintained in the southern part during the northeast monsoon. This means that the heavy northeast monsoon rain is of no importance in reducing the salinity in the southern part of the Strait of Malacca.

In the northern part of the Strait, the situation is different. The salinity changes in accordance with changing rainfall, as shown in Fig. 1. The tidal currents seem also to play an important role in reducing the salinity. The quantities of fresh water flowing from the rivers of East Sumatra and West Malacca are mixed gradually by the effect of the strong tidal currents. According to the available data, there is an increase in velocity of the northwest-going current during the northeast monsoon. This current accelerates the transfer of the watermass with low salinity from the southern part to the northern part of the Strait, reducing the salinity in the middle and northern parts to a minimum in December.

During the transition period of March-April, the northeast monsoon gradually decreases in strength and is finally replaced by the southwest monsoon. The current from the South China Sea reaches its maximum velocity, and the $30.5^0/_{00}$ isohaline moves to the north. The penetration of higher saline water from the South China Sea causes a maximum in the northern part in March.

During the southwest monsoon period of May-September, a northerly current adduces the $31.0^0/_{00}$ - $32.0^0/_{00}$ Java Sea water, which forms a minimum value in salinity in the centre of the Java Sea during the whole year, through the Gaspar and Karimata Straits into the South China Sea. This watermass reaches its maximum advance in the centre of the southern part of South China Sea at lat. 1° N. in August, and seems not to flow into the Strait of Malacca. At the east coast of Sumatra a watermass of low salinity is formed by runoff of the various big rivers. This watermass with salinities below $30.0^0/_{00}$ is pushed through the narrow straits between the many islands of the southern entrance into the Malacca Strait in a northwesterly direction. According to the Current Atlas, there is a southeast-going current in the narrowest part of the Strait in about June and August. This means that fresh water flowing from the rivers of East Sumatra and West Malacca, south of lat. 3° N., reduces the south-

east-going current. The low saline watermasses, flowing from the southeast and from the northwest, meet in the southern entrance of the Strait and form a front between longs. 104° E. - 105° E. and lats. 0° - 1° N. during June-August. From then onwards, the front thus formed slowly moves northwestward, mixes with watermasses in the inner part of the Strait, emerging further into the Indian Ocean. It is probable that this could be one of the important factors in reducing the salinity in the southern part, in spite of less rain. The decrease in salinity starts in the coastal region of East Sumatra, advancing gradually to the southpoint of Malay peninsula. This could be attributed to the greater landdrainage from the rivers of East Sumatra than that from the rivers of West Malacca.

In the northern and central parts of the Malacca Strait, a decrease in salinity is noted in May. This is in accordance with the slight increase in rainfall after February. Besides, the high velocity of the northwest-going current during March-April, accelerates the transfer of low saline water from the inner part of the Strait into the northern part, which water also helps in lowering the salinity in the latter region to a minimum in May. A sudden increase in salinity starting after May, to the maximum in August, after which it decreases again to a minimum in December, also coincides with the slight drop in rainfall from May to August, after which it increases to a maximum in December. Whilst discussing the Malacca Strait, K.M. WEEL (1923) stated that, in August, the salinities in the Strait of Malacca gradually increased from South to North and that this was a consequence of the unimportant discharge of fresh water from the rivers into the Strait, of the weak northwest-going current, and of the strong tidal streams. This increase in salinity in the Malacca Strait from South to North starting in June and ending in September, is also noted by the writer.

The lowest salinities in the northern part of the Strait of Malacca are found along the Malacca shore throughout the year, and increase towards the east coast of Sumatra. This phenemenon seems to be caused by the northwest-going current being stronger along the west coast of Malacca than that along the east coast of Sumatra. This would push the low saline watermass from the inner part of the Strait more towards the west coast of Malacca.

The 30.5‰ isohaline, as seen in the isopleths between lats. 3° N. - 4° N., separates two watermasses. The one, which occupies the middle and northern parts of the Malacca Strait has two salinity maxima and

two salinity minima, while the other, covering the southern part of the Strait, has only one salinity maximum and one salinity minimum.

The isopleths show two types of northwesterly watermovements in the Strait of Malacca, one as a result of the northeast monsoon transporting high saline water from the South China Sea into the Strait, the other as a result of the southwest monsoon transporting low saline water from the coastal region of East Sumatra into the Strait.

Acknowledgments

Acknowledgment is given to the Officers of the several private navigation companies and to the government Navigation Services which operate regularly in the Strait of Malacca, for their voluntary coöperation in taking the watersamples.

Sincerest thanks are due to Dr. K. Wyrtki oceanographer of the Lembaga Penjelidikan Laut at Djakarta and to Mr. E. H. Dahlgren fishery adviser to the I.C.A. in Indonesia, for their many helpful criticisms and suggestions in preparing this paper.

Finally to Mr. P. Ch. Veen former oceanographer of the Lembaga Penjelidikan Laut at Djakarta for his keen interest in collecting most of the data used in this paper.

References

Berlage, Jr. H. P., 1949. Regenval in Indonesië (Rainfall in Indonesia) Koninklijke Magnetisch en Meteorologisch Observatorium te Batavia. Verhandelingen No. 37, 1949.

Hydrographic Department, Admiralty, 1946.Malacca Strait Pilot 1946.

Tham Ah Kow, 1953. A preliminary study of the physical, chemical and biological characteristics of Singapore Straits. Fishery publication Singapore Vol. 1 No. 4, 1953.

U. S. Navy Hydrographic Office, 1944. Atlas of surface currents Indian Ocean 1950.

Veen, P. Ch., 1953. Preliminary charts of the mean salinity of the Indonesian Archipelago and adjacent waters. Organization for Scientific Research in Indonesia. Bulletin No. 17, 1953.

Weel, K. M., 1923. Meteorological and Hydrographical observations made in the western part of the Netherlands East Indian Archipelago. Treubia, Mai 1923.

Wyrtki, K., 1956. Monthly charts of surface salinity in Indonesian and adjacent waters. Journ. du Conseil Vol. XXI No. 3, 1956.

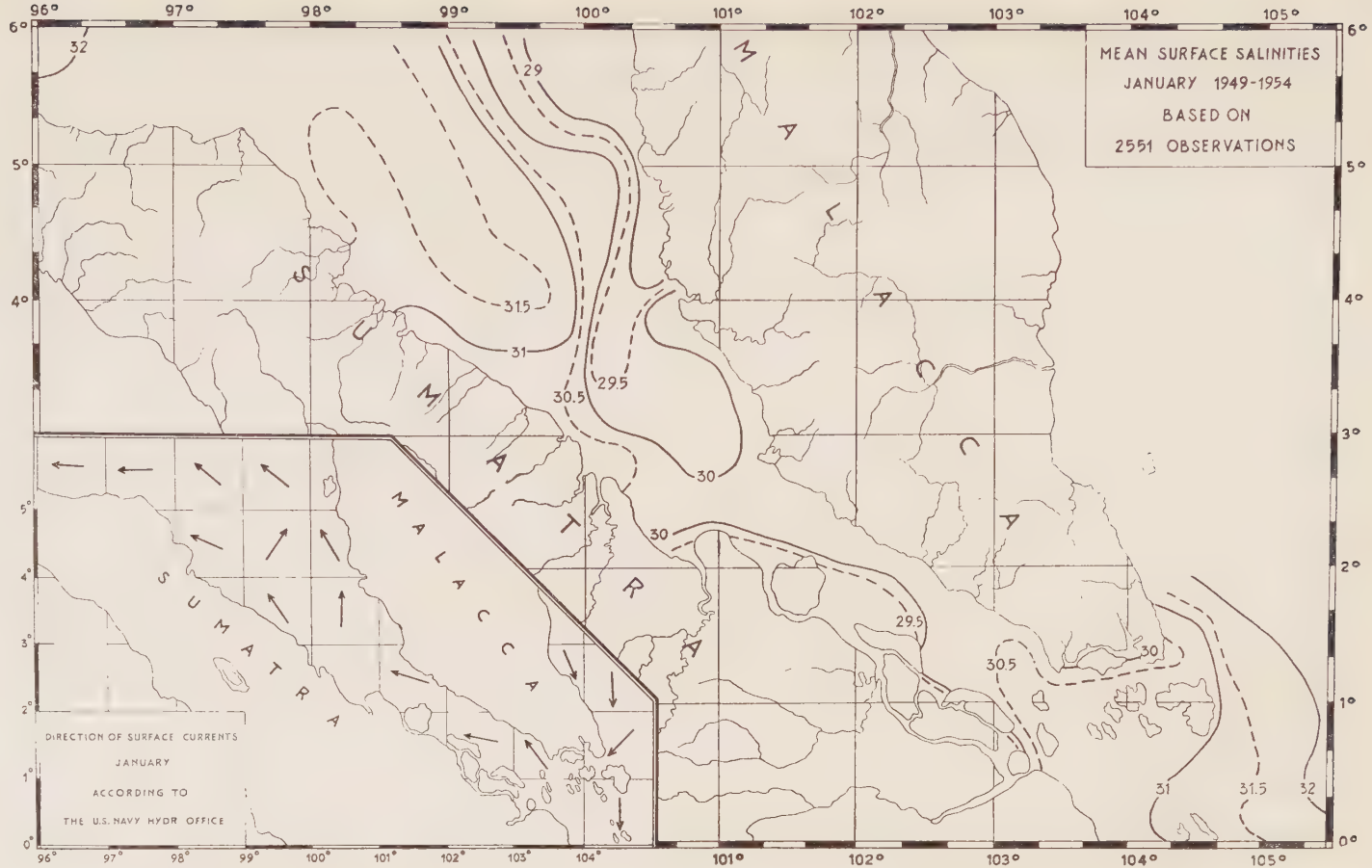
MEAN SURFACE SALINITIES
JANUARY 1949-1954
BASED ON
2551 OBSERVATIONS
DIRECTION OF SURFACE CURRENTS
JANUARY
ACCORDING TO
THE U.S. NAVY HYDR OFFICE
SUMATRA
MALACCA
MALACCA
32
29
31.5
31
30.5
29.5
30
30
29.5
30.5
30
31
31.5
32
96°
97°
98°
99°
100°
101°
102°
103°
104°
105°
6°
5°
4°
3°
2°
1°
0°

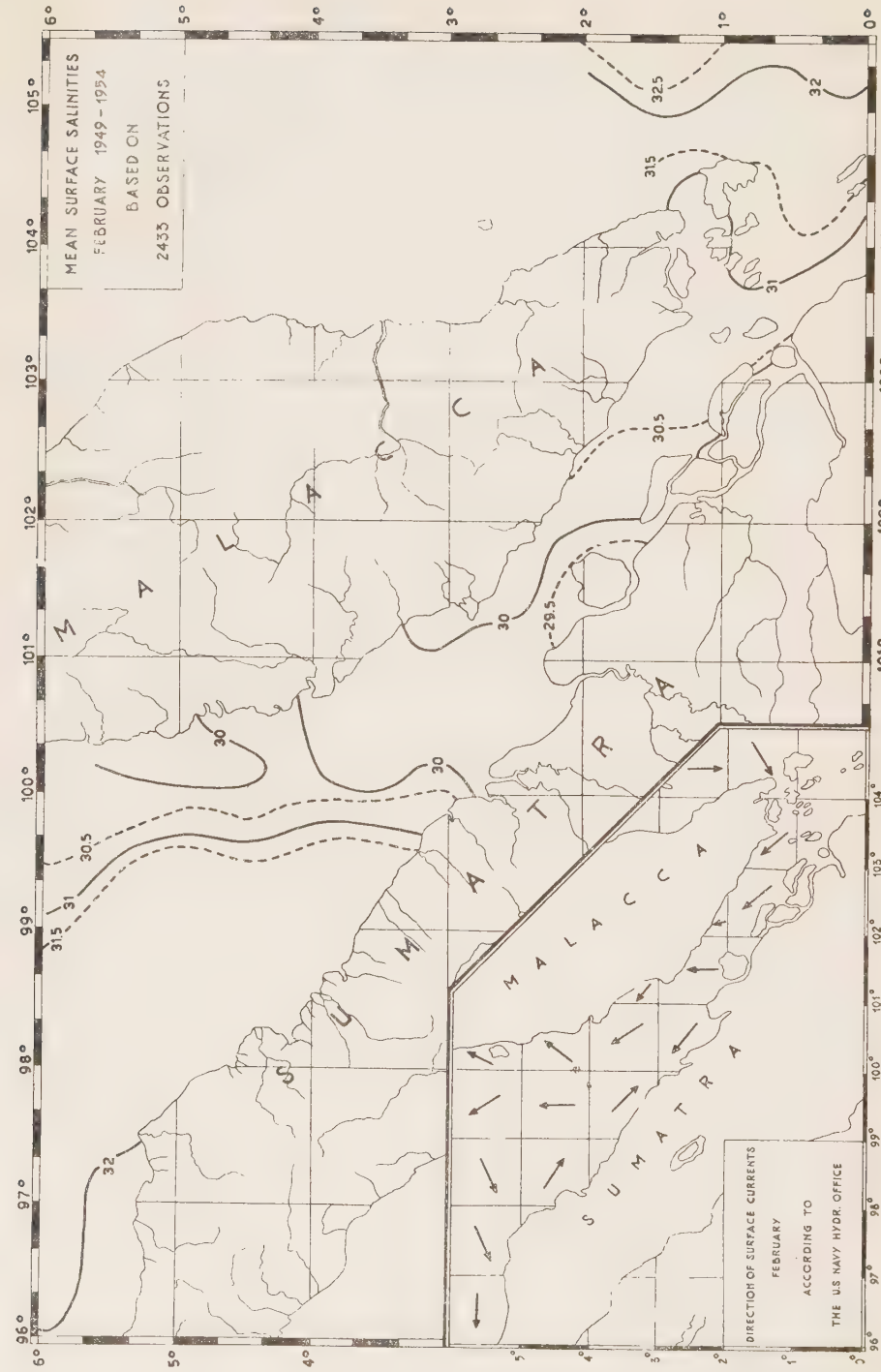
MEAN SURFACE SALINITIES
FEBRUARY 1949 - 1954
BASED ON
2433 OBSERVATIONS
DIRECTION OF SURFACE CURRENTS
FEBRUARY
ACCORDING TO
THE U.S. NAVY HYDR. OFFICE
MALACCA
SUMATRA
30
30.5
31
31.5
32
29.5
325
315

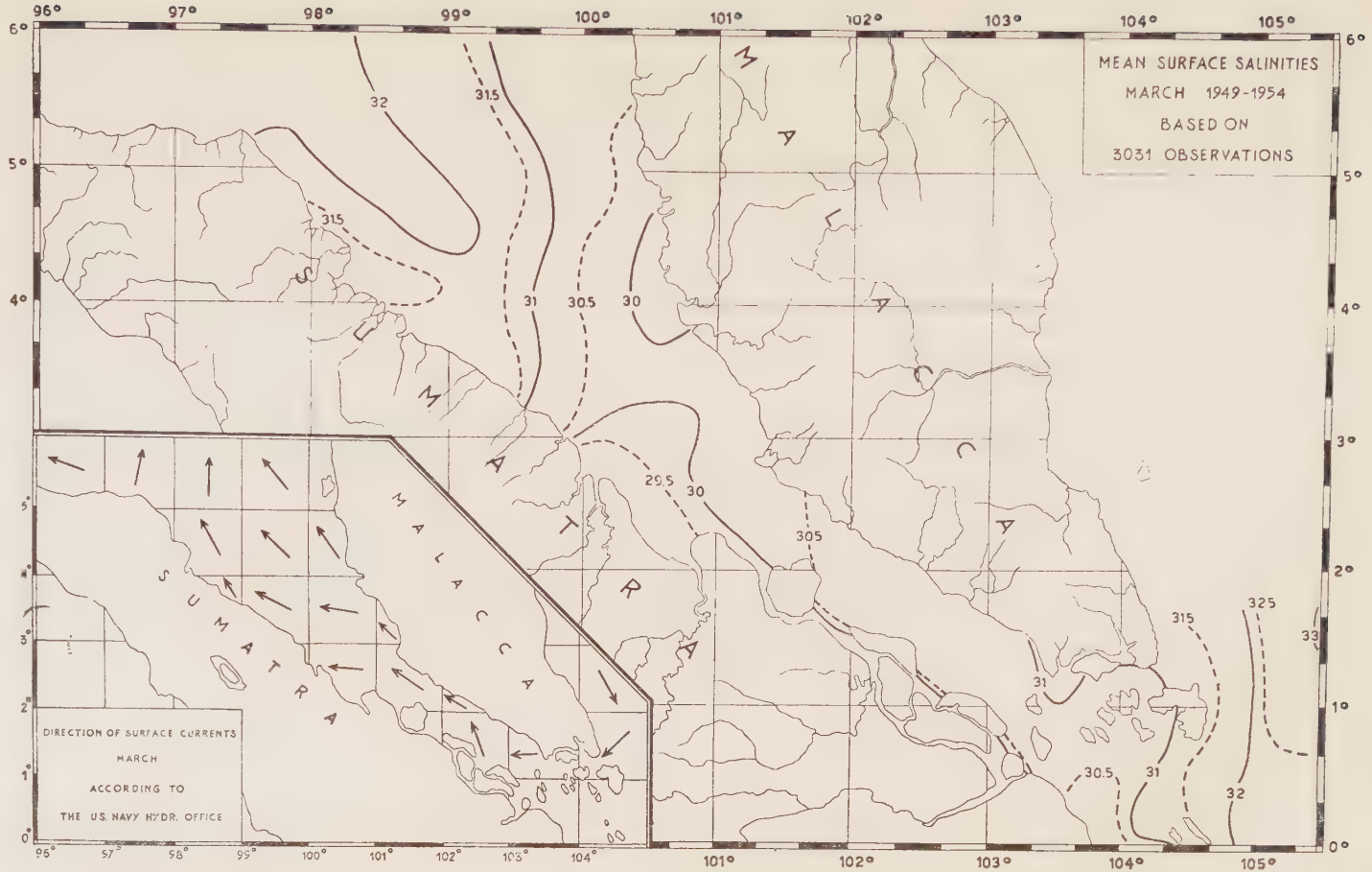
MEAN SURFACE SALINITIES
MARCH 1949-1954
BASED ON
3031 OBSERVATIONS
DIRECTION OF SURFACE CURRENTS
MARCH
ACCORDING TO
THE U.S. NAVY HYDR. OFFICE
SUMATRA
MALACCA
STRAITS
MALACCA
32
31.5
31.5
31
30.5
30
29.5
30
30.5
31
31.5
32
32.5
33
96°
97°
98°
99°
100°
101°
102°
103°
104°
105°
6°
5°
4°
3°
2°
1°
0°

MEAN SURFACE SALINITIES
APRIL 1949-1954
BASED ON
2888 OBSERVATIONS
MALACCA STRAIT
SUMATRA
MALACCA
DIRECTION OF SURFACE CURRENTS
APRIL
ACCORDING TO
THE U.S. NAVY HYDR. OFFICE

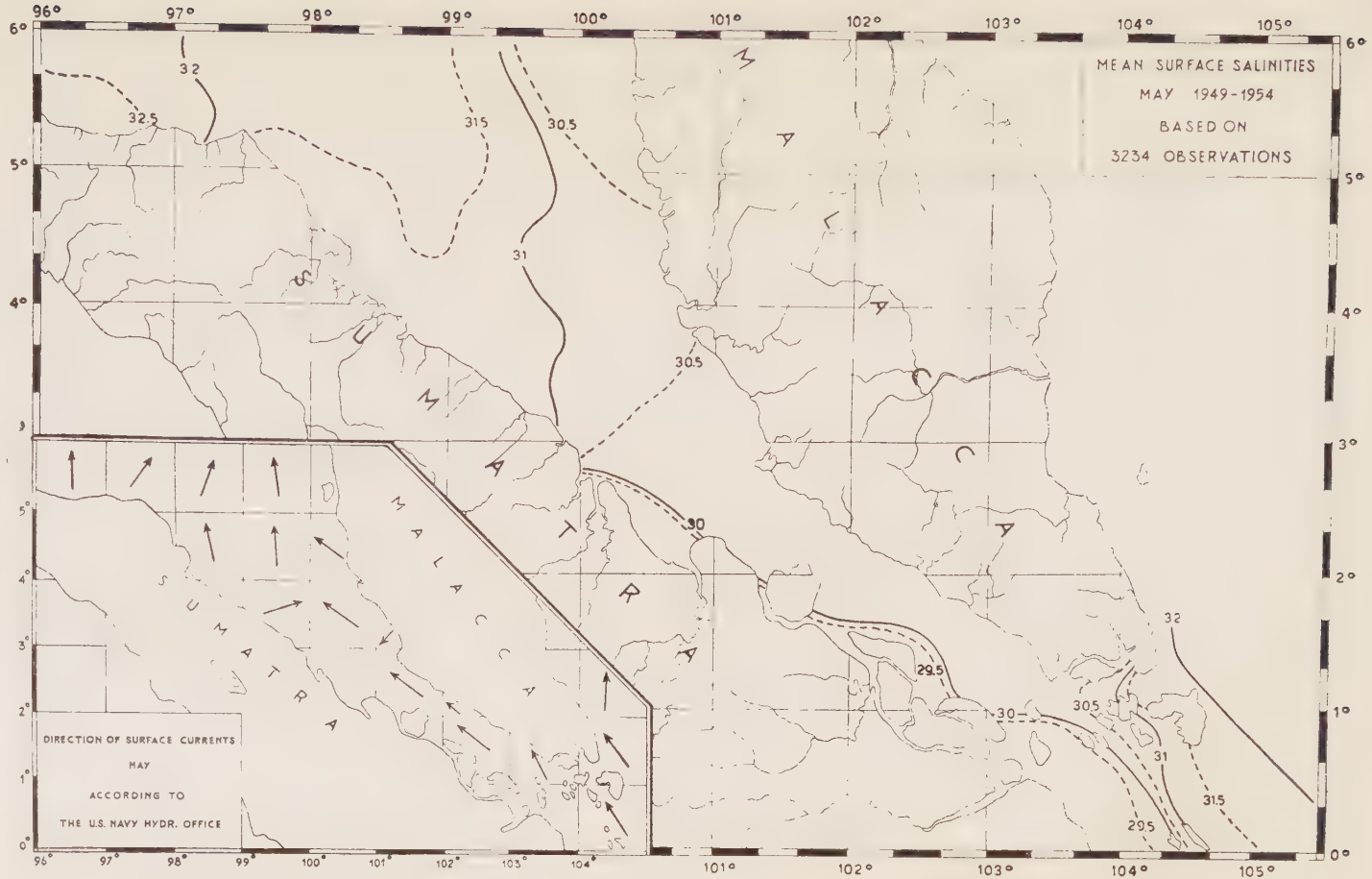
MEAN SURFACE SALINITIES
MAY 1949-1954
BASED ON
3234 OBSERVATIONS
DIRECTION OF SURFACE CURRENTS
MAY
ACCORDING TO
THE U.S. NAVY HYDR. OFFICE
SUMATRA
MALACCA
MALACCA
32
32.5
31.5
30.5
31
30.5
30
29.5
30
30.5
32
31
31.5
29.5
96°
97°
98°
99°
100°
101°
102°
103°
104°
105°
6°
5°
4°
3°
2°
1°
0°

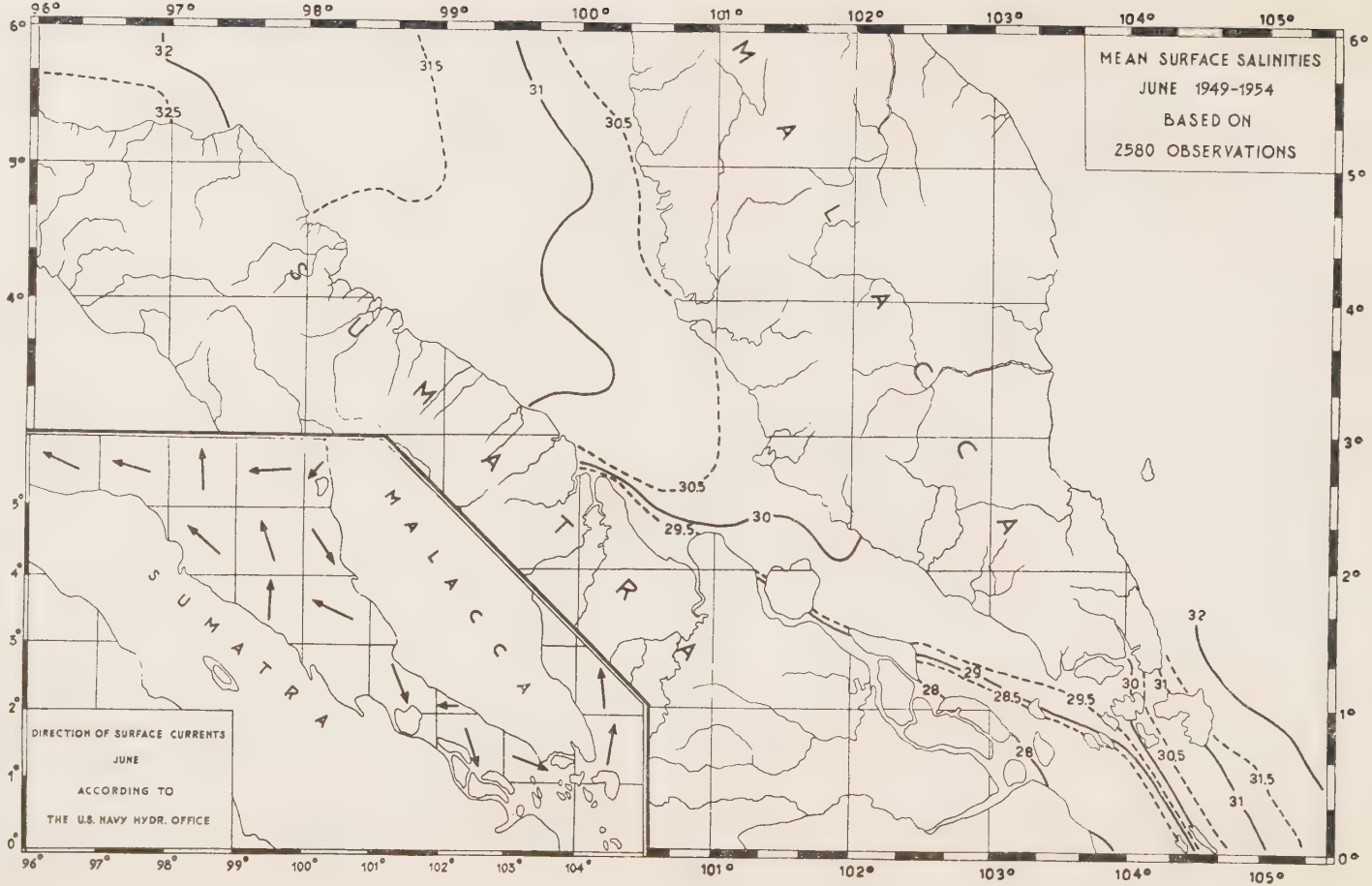
MEAN SURFACE SALINITIES
JUNE 1949-1954
BASED ON
2580 OBSERVATIONS
DIRECTION OF SURFACE CURRENTS
JUNE
ACCORDING TO
THE U.S. NAVY HYDR. OFFICE
SUMATRA
MALACCA
STRAIT
MALACCA
32
31.5
325
31
30.5
30
29.5
29
28.5
28
96°
97°
98°
99°
100°
101°
102°
103°
104°
105°
6°
5°
4°
3°
2°
1°
0°

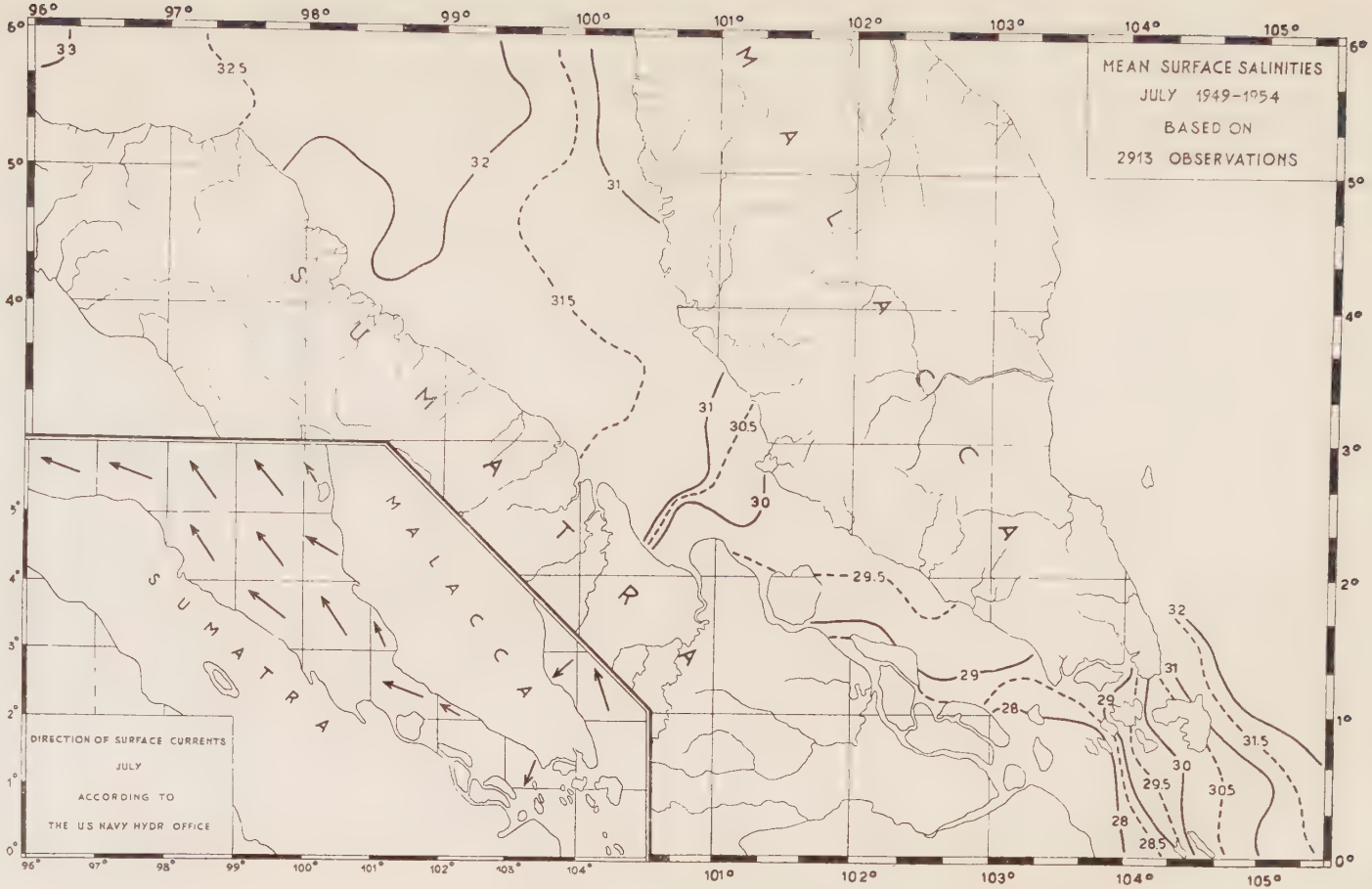
MEAN SURFACE SALINITIES
JULY 1949-1954
BASED ON
2913 OBSERVATIONS
DIRECTION OF SURFACE CURRENTS
JULY
ACCORDING TO
THE U.S NAVY HYDR OFFICE
SUMATRA
MALACCA
MALACCA
96°
97°
98°
99°
100°
101°
102°
103°
104°
105°
6°
5°
4°
3°
2°
1°
0°
33
32.5
32
31
31.5
30.5
30
29.5
29
28.5
28
31.5
30.5

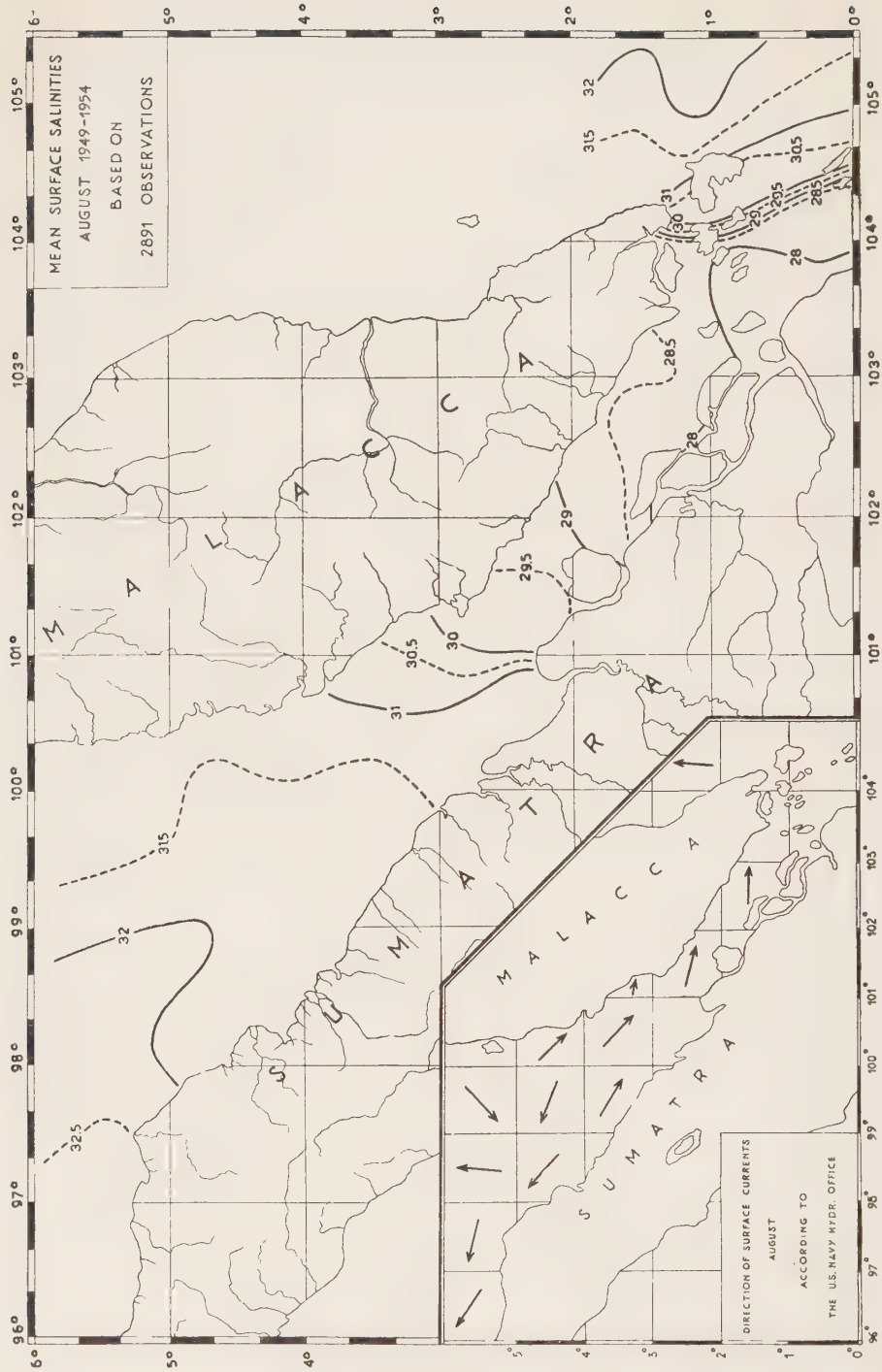
MEAN SURFACE SALINITIES
AUGUST 1949-1954
BASED ON
2891 OBSERVATIONS
MALACCA STRAIT
MALACCA
SUMATRA
DIRECTION OF SURFACE CURRENTS
AUGUST
ACCORDING TO
THE U.S. NAVY HYDR. OFFICE

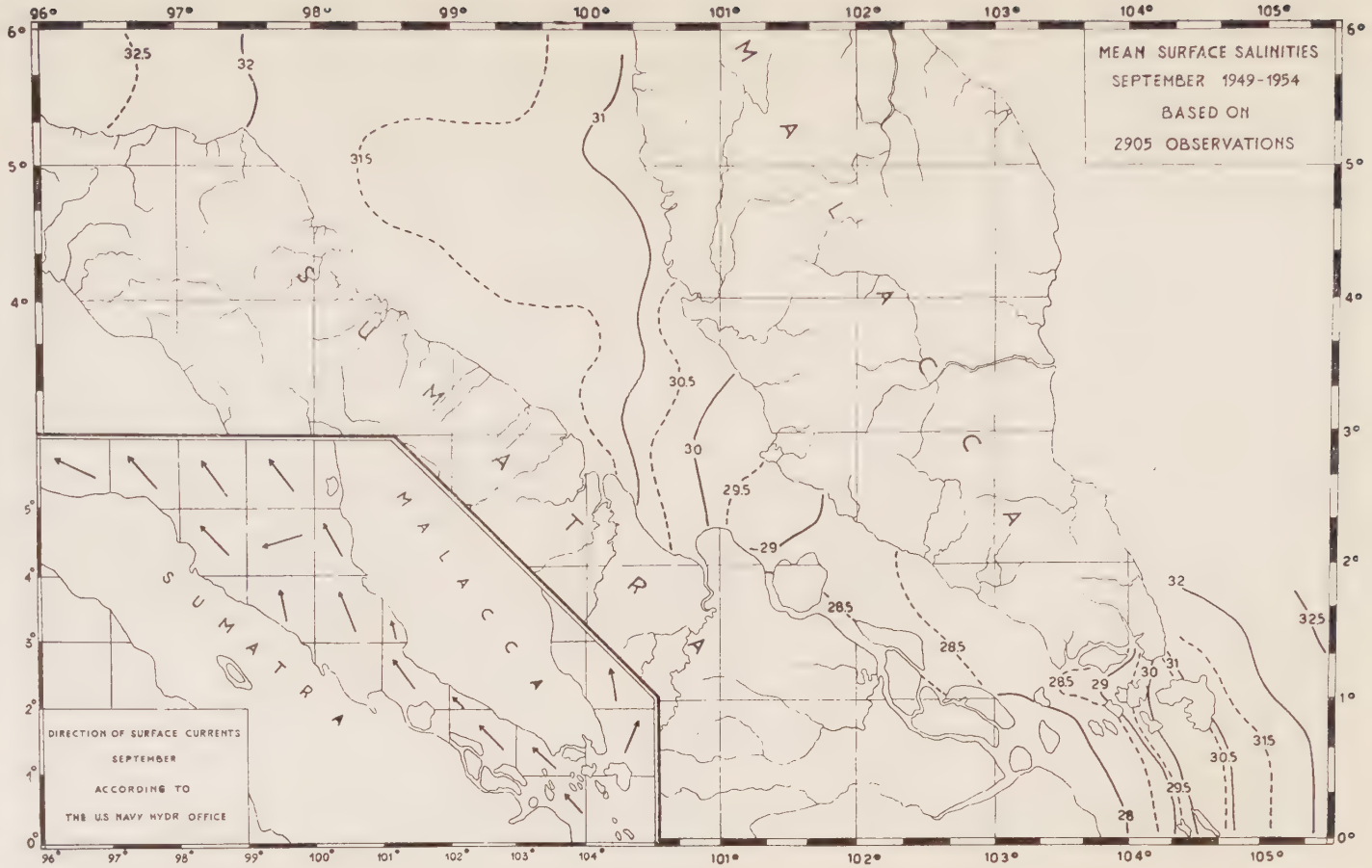
MEAN SURFACE SALINITIES
SEPTEMBER 1949-1954
BASED ON
2905 OBSERVATIONS
DIRECTION OF SURFACE CURRENTS
SEPTEMBER
ACCORDING TO
THE U.S NAVY HYDR OFFICE
SUMATRA
MALACCA
MALACCA
96°
97°
98°
99°
100°
101°
102°
103°
104°
105°
6°
5°
4°
3°
2°
1°
0°
32.5
32
31.5
31
30.5
30
29.5
29
28.5
28

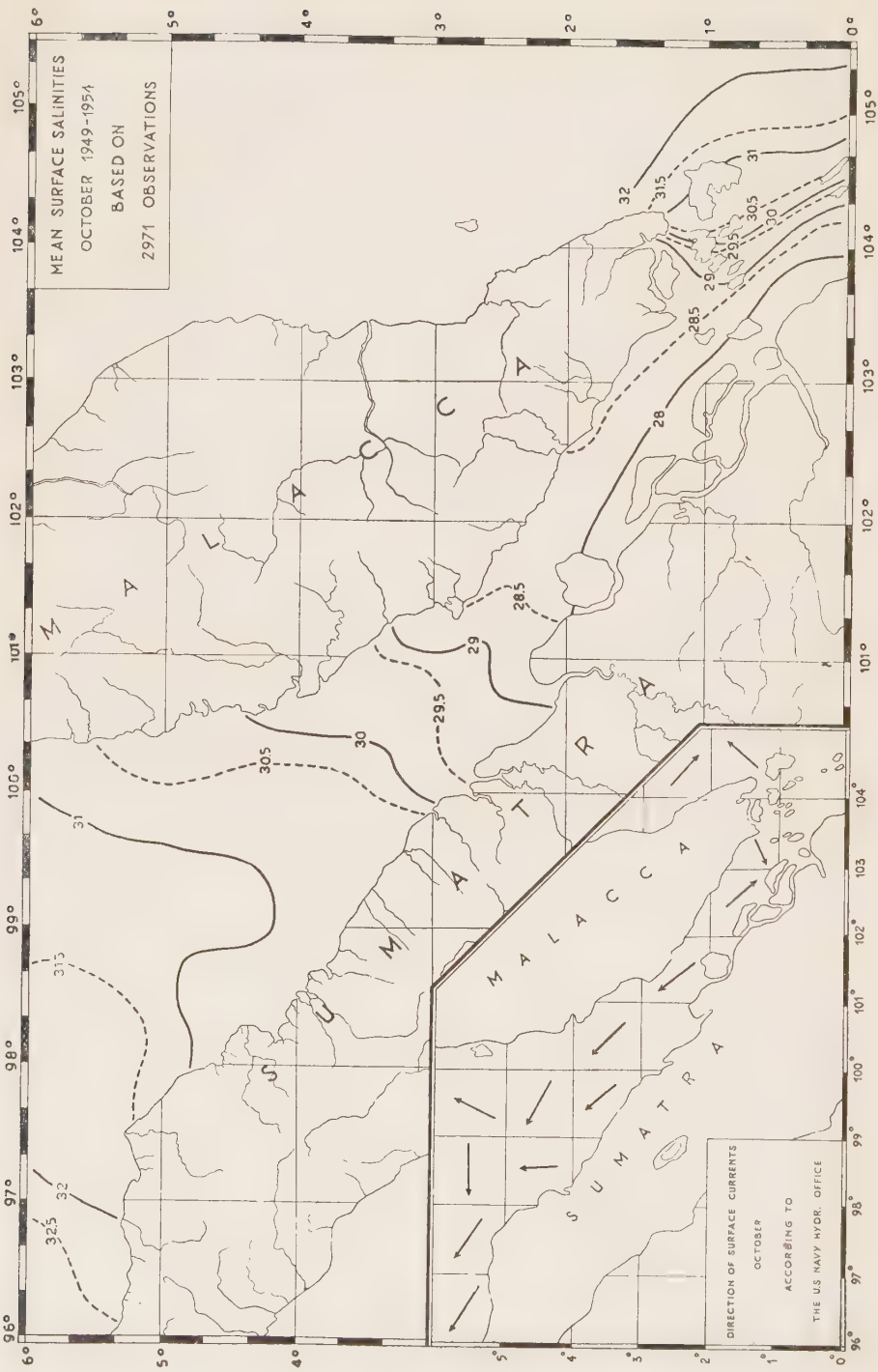
MEAN SURFACE SALINITIES
OCTOBER 1949-1954
BASED ON
2971 OBSERVATIONS
DIRECTION OF SURFACE CURRENTS
OCTOBER
ACCORDING TO
THE U.S. NAVY HYDR. OFFICE
MALACCA
SUMATRA
SUMATRA
PENINSULA
MALAYA
32
31.5
31
30.5
30
29.5
29
28.5
28
32.5
31.5
31
30.5
30
29.5
29
28.5
28

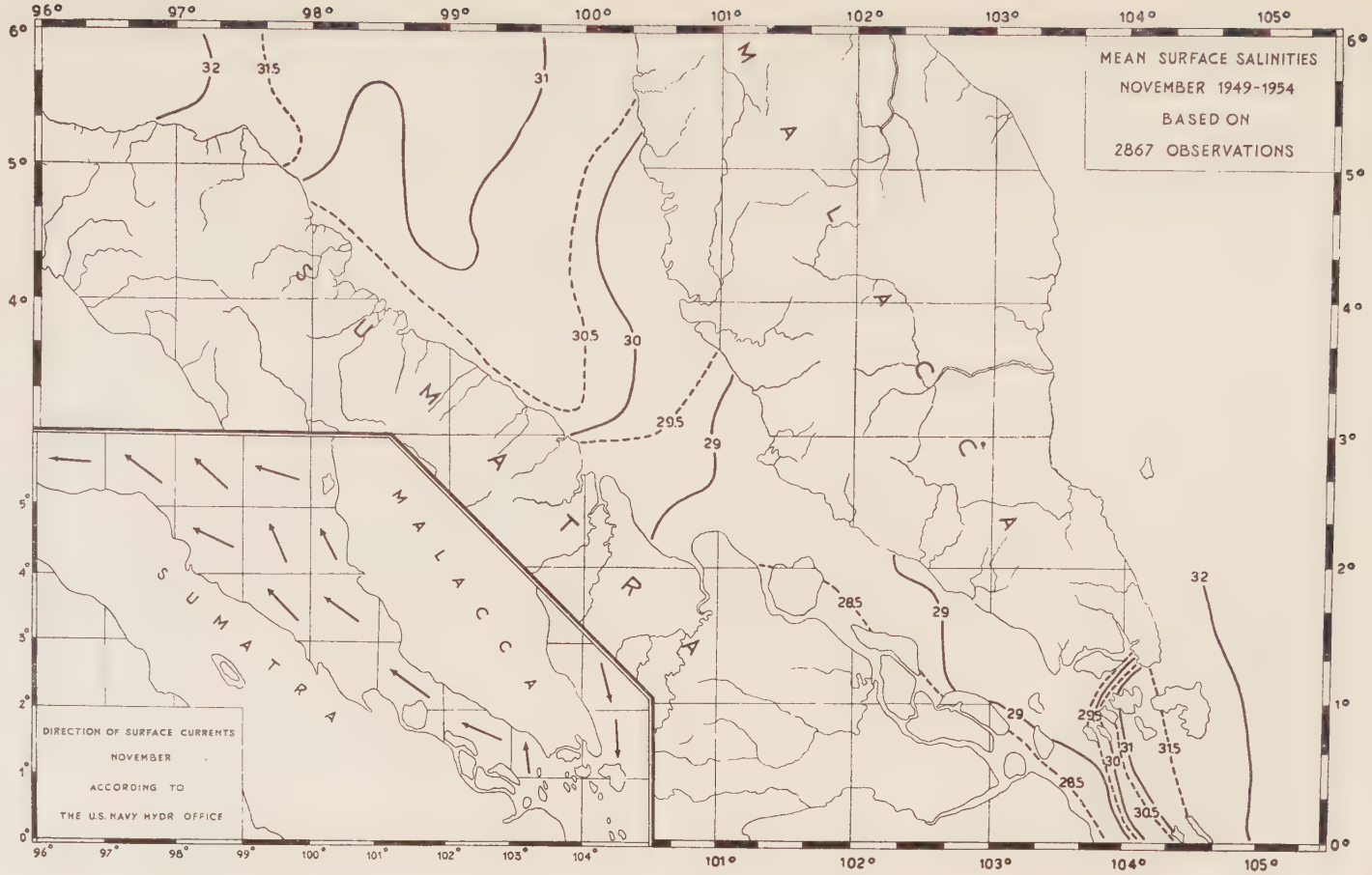
MEAN SURFACE SALINITIES
NOVEMBER 1949-1954
BASED ON
2867 OBSERVATIONS
DIRECTION OF SURFACE CURRENTS
NOVEMBER
ACCORDING TO
THE U.S. NAVY HYDR OFFICE
SUMATRA
MALACCA
MALACCA
32
31.5
31
30.5
30
29.5
29
28.5
29
29.5
31
31.5
30
30.5
28.5
32
96°
97°
98°
99°
100°
101°
102°
103°
104°
105°
6°
5°
4°
3°
2°
1°
0°

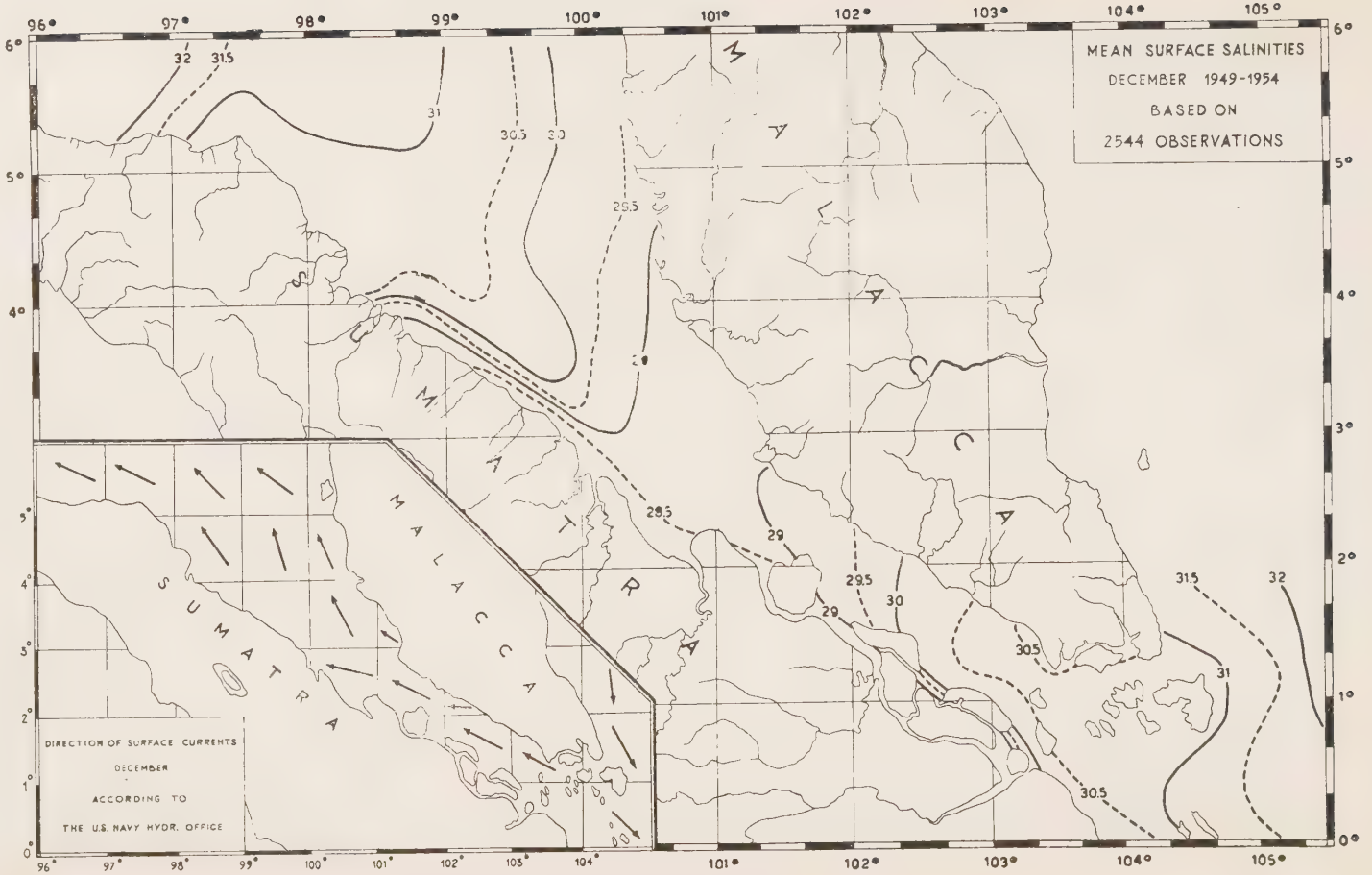
MEAN SURFACE SALINITIES
DECEMBER 1949-1954
BASED ON
2544 OBSERVATIONS
DIRECTION OF SURFACE CURRENTS
DECEMBER
ACCORDING TO
THE U.S. NAVY HYDR. OFFICE
SUMATRA
MALACCA
MALAYA
32
31.5
31
30.5
30
29.5
29
28.5
96°
97°
98°
99°
100°
101°
102°
103°
104°
105°
6°
5°
4°
3°
2°
1°
0°

Oceanographic Station List 1956

Oceanographic stations obtained by research vessel *Samudera* in 1956 in the Java Sea, the Flores Sea, the Celebes Sea and the waters around the island Halmahera.

Depth in meters, **fat meters** refer to thermometric depth. Temperatures in Centigrade, corrected, Salinities in $^0/_{00}$, Oxygen in ml/liter.

Station 1. 15-1-1956, 1200h
3° 03′ S. 107° 19′ E.
Depth: 53 m. Wind: N 3

m	t	S	O_2
0	27,0	31,89	—
10	27,40	32,36	4,56
20	27,37	32,34	—
30	27,38	32,34	—
40	27,37	32,34	—
50	27,38	32,34	4,50

Station 2. 16-1-1956 1200h
1° 50′ S. 108° 38′ E.
Depth: 42 m. Wind: N 3-4

m	t	S	O_2
0	27,7	32,79	—
10	27,35	32,77	4,52
20	27,30	32,77	—
30	27,30	32,75	—
40	27,32	32,68	4,69

Station 3. 17-1-1956 10.00h
3° 34′ S. 109° 10′ E.
Depth: 46 m. Wind: W 4.

m	t	S	O_2
0	27,2	32,52	—
10	27,30	32,86	4,61
20	27,33	32,86	—
30	27,34	32,86	4,53
40	27,31	32,91	4,66

Station 4. 17-1-1956 1900h
3° 45′ S. 110° 15′ E.
Depth: 34 m. Wind: W 3.

m	t	S	O_2
0	27,6	31,46	—
10	27,57	31,33	4,65
20	27,62	31,34	—
30	27,62	31,33	4,69

Station 5. 18-1-1956 0830h
4° 10′ S. 111° 55′ E.
Depth: 35 m. Wind: W 3.

m	t	S	O_2
0	27,4	31,51	—
5	27,56	31,41	—
10	27,71	31,44	4,75
15	27,40	31,37	—
20	27,41	31,40	—
25	27,43	31,44	—
30	27,44	31,46	4,71

Station 6. 18-1-1956 1800h
4° 30′ S. 113° 23′ E.
Depth: 48 m. Wind: W 1.

m	t	S	O_2
0	27,7	31,20	—
5	27,90	31,15	—
10	27,70	31,15	4,59
15	27,43	31,16	—
20	27,40	31,19	—
25	27,34	31,20	—
30	27,41	31,20	—
35	27,60	31,22	—
40	27,47	31,22	4,61
45	—	31,19	—

Station 7. 19-1-1956 0600h
4° 43′ S. 115° 18′ E.
Depth: 28 m. Wind: 0

m	t	S	O_2
0	27,7	30,97	—
5	27,79	30,86	—
10	27,75	31,09	4,73
15	27,70	31,22	—
20	27,68	31,29	—
25	27,62	31,31	4,52

Station 8. 19-1-1956 1900h
4° 49′ S. 117° 03′ E.
Depth: 48 m. Wind: 0

m	t	S	O_2
0	28,4	31,91	—
10	28,32	31,83	4,70
20	28,16	31,89	—
30	28,11	31,91	—
40	28,10	31,94	4,46
45	28,10	32,00	—

Station 9. 20-1-1956 0600-0700h
5° 01′ S. 118° 01′ E.
Depth: 1200 m. Wind: E 1.

m	t	S	O_2
0	28,1	32,36	—
20	28,09	32,38	4,51
40	28,18	32,54	—
60	27,70	33,13	—
80	27,17	33,58	—
100	26,14	34,03	3,84
120	20,97	34,63	3,50
140	18,26	34,71	3,57
160	17,65	34,72	3,49
180	17,51	34,72	3,48
200	—	34,71	3,36
250	13,61	34,54	3,08
300	10,40	34,48	2,69
350	9,37	34,49	2,64
400	8,93	23,49	2,49
500	(8,00)	34,56	2,44

Station 10. 20-1-1956 1100-1200h
5° 03′ S. 118° 34′ E.
Depth: 800 m. Wind: E 1.

m	t	S	O_2
0	28,8	32,30	—
20	28,17	32,36	4,55
40	28,12	32,61	—
60	27,90	32,95	—
80	27,10	33,77	—
100	24,10	34,54	3,81
120	21,97	34,72	3,74
140	19,67	34,77	3,70
160	18,96	34,76	3,49
180	16,02	34,73	3,47
200	15,90	—	3,49
250	11,44	34,49	2,89
300	10,30	34,42	2,74
350	8,95	34,48	2,48
400	8,39	34,49	2,35
500	7,19	34,52	2,46

Station 11. 20-1-1956 1530-1630h
5° 06′ S. 118° 56′ E.
Depth: 510 m. Wind: N 2

m	t	S	O_2
0	28,4	32,56	—
20	28,24	32,47	4,67
40	28,24	32,41	—
60	27,90	32,63	—
80	23,81	34,54	—
100	21,97	34,63	3,76
120	21,02	34,74	—
140	20,66	34,78	3,69
160	20,28	34,79	—
180	16,90	34,65	—
200	14,80	34,67	3,16
250	12,53	34,56	—
300	11,04	34,51	2,70
350	9,30	34,49	2,53
400	7,80	34,49	2,46
500	6,75	34,52	2,41

Station 12. 23-1-1956 2200-2300h
5° 44′ S. 118° 38′ E.
Depth: 870 m. Wind: NW 2

m	t	S	O_2
0	28,2	32,18	—
20	28,18	32,18	4,69
40	28,22	32,36	—
60	28,09	32,74	—
80	25,66	34,20	—
100	24,32	34,47	4,04
120	21,59	34,76	3,82
140	19,70	34,76	3,79
160	19,13	34,76	3,75
250	13,22	34,56	3,15

Station 13. 24-1-1956 04-06h
6° 15′ S. 118° 35′ E.
Depth: 360 m. Wind: W 3-4

m	t	S	O_2
0	28,1	32,03	—
20	28,10	32,18	4,77
40	27,40	33,08	—
60	25,76	33,89	—
80	24,23	34,27	—
100	22,39	34,65	3,85
114	21,06	34,65	3,77
133	19,57	34,70	3,72
152	18,95	34,70	3,72
170	17,70	34,69	3,56
190	16,31	34,65	3,47
230	14,35	34,54	3,35
253	13,61	34,54	3,15
276	12,42	34,47	3,01
299	11,34	34,47	2,94
322	9,60	34,41	2,59

Station 14. 24-1-1956 10h-12h
6° 32′ S. 118° 17′ E.
Depth: 285 m. Wind: W 2-3

m	t	S	O_2
0	28,3	32,01	—
20	28,09	31,92	4,56
40	28,10	32,10	—
60	27,20	33,08	—
80	25,48	33,80	—
100	21,89	34,65	3,69
120	20,21	34,70	3,78
140	18,37	34,70	3,64
160	17,74	34,70	—
180	16,64	34,69	3,60
200	15,40	34,61	3,49
225	14,30	34,54	3,49
250	13,01	34,40	3,14
280	11,97	—	2,99

Station 15. 24-1-1956 18-1930h
6° 40′ S. 117° 26′ E.
Depth: 380 m. Wind: W 2-3

m	t	S	O_2
0	28,0	32,25	—
20	28,07	32,19	4,83
40	27,88	32,52	—
60	27,82	32,50	—
80	26,00	33,16	—
100	25,48	33,93	4,22
120	21,37	34,58	3,80
140	20,31	34,67	3,71
160	18,71	34,72	3,67
180	16,90	34,65	3,55
200	15,27	34,65	3,53
230	14,18	34,61	3,41
280	11,80	34,54	3,02
325	9,88	34,51	2,61
350	9,39	34,49	2,48

Station 16. 25-1-1956 0100-0240h
6° 45′ S. 116° 46′ E.
Depth: 600 m. Wind: SW 2-3

m	t	S	O_2
0	28,2	32,22	—
20	28,14	32,21	4,30
40	28,20	32,21	—
60	28,00	32,55	—
80	27,91	32,70	—
100	24,52	34,23	3,91
120	20,08	34,66	3,75
140	16,55	34,71	3,49
160	15,80	34,67	3,39
180	15,10	34,61	3,44
200	14,61	34,59	3,32
250	13,76	34,60	3,31

Station 17. 26-1-1956 17.00h
6° 33′ S. 112° 05′ E.
Depth: 46 m. Wind: W 3

m	t	S	O_2
0	27,75	32,06	—
10	27,84	32,01	—
20	27,88	31,95	—
30	27,88	31,96	—
40	27,90	31,90	—

Station 18. 27-1-1956 12.00h
6° 09′ S. 109° 20′ E.
Depth: 50 m. Wind: W 2

m	t	S	O_2
0	27,4	31,86	—
10	27,42	31,86	—
20	27,42	31,88	—
30	27,43	31,92	—
40	27,41	31,99	—
50	27,41	32,02	—

Station 19. 12-6-1956 0730-0900h
7° 52′ S. 116° 30′ E.
Depth: 1500 m. Wind: SE 2

m	t	S	O_2
0	28,7	32,72	—
20	28,66	32,68	4,54
50	27,84	33,69	4,34
65	26,39	34,20	3,92
80	25,93	34,25	4,04
95	25,24	34,36	4,05
115	24,60	34,43	3,87
132	23,45	34,61	3,88
150	21,38	—	3,56
167	19,67	34,61	3,49
210	14,57	34,61	3,27
250	12,30	34,54	3,00
335	10,36	34,49	2,68
450	10,05	34,49	2,58
550	—	34,56	2,32
650	6,48	34,58	2,30
750	5,71	34,58	2,06
850	5,20	34,56	2,14
950	4,77	34,58	2,15

Station 20, 12-6-1956 2000-2130h
6° 58′ S. 117° 43′ E.
Depth: 510 m. Wind: E 2

m	t	S	O_2
0	28,6	33,40	—
18	28,60	33,21	4,69
36	28,37	33,37	4,70
54	28,09	33,60	4,64
72	26,61	34,05	4,39
90	25,62	34,40	3,95
110	23,71	34,49	3,89
140	21,63	34,70	—
160	19,59	34,67	3,61
180	18,49	34,69	—
200	16,91	34,63	3,45
250	14,88	34,60	3,39
280	12,59	34,49	3,11
300	11,82	34,49	2,99
320	10,30	34,42	2,69
420	8,90	34,43	2,45

Station 21. 13-6-1956 1200-1400h
5° 41′ S. 118° 56′ E.
Depth: 1010 m. Wind: E 3-4

m	t	S	O_2
0	28,1	33,77	—
20	27,60	34,00	4,65
40	25,87	34,36	4,28
60	24,79	34,54	4,07
80	24,63	34,56	3,95
100	24,64	—	—
120	22,22	34,72	3,81
140	22,29	34,69	3,81
160	20,90	34,74	3,61
180	20,11	34,69	3,68
200	19,19	34,69	3,59
250	16,42	34,63	3,37
300	11,84	34,52	2,95
360	10,07	34,47	2,89
455	8,70	34,49	2,45
550	7,47	34,51	2,46
645	6,38	34,54	2,41
740	5,98	—	—
830	5,32	34,54	2,30

Station 22. 19-6-1956 1700-1900h
1° 10′ N. 122° 40′ E.
Depth: > 2000 m. Wind: E 1

m	t	S	O_2
0	29,8	33,98	—
20	28,31	34,13	4,54
40	27,37	34,38	4,62
60	26,82	34,38	4,55
80	25,77	34,42	4,19
100	22,27	34,72	3,90
120	20,40	34,76	3,74
140	20,37	34,79	3,80
160	19,02	34,76	3,71
180	18,26	34,74	3,77
200	17,15	34,67	3,68
250	13,06	34,51	3,33
300	12,29	34,43	3,27
400	9,34	34,49	2,70
500	7,64	34,51	2,64
600	6,84	34,54	2,56
700	6,21	34,52	2,52

800	5,74	—	—
900	5,15	34,54	2,36
1080	4,53	34,56	2,24
1280	3,96	34,60	2,33

Station 23. 22-6-1956 1600-1800h
1° 06′ N. 126° 32′ E.
Depth: 1800 m. Wind: NE 2

m	t	S	O_2
0	29,5	33,48	—
20	29,37	33,89	5,20
40	28,73	33,98	4,62
60	28,17	34,02	4,77
80	26,92	34,27	4,42
100	25,70	34,56	4,34
120	24,16	34,61	4,31
140	22,03	34,73	3,99
160	20,96	34,76	3,93
180	16,63	34,67	3,66
200	16,04	34,65	—
250	12,61	34,56	3,14
300	11,74	34,58	2,94
400	9,98	34,54	2,91
500	7,69	34,58	2,46
570	6,87	34,54	2,50
670	6,15	34,56	2,58
765	5,61	34,56	2,57
860	5,16	34,54	2,55
960	4,55	34,56	2,43
1160	3,86	34,61	2,44

Station 24. 24-6-1956 0800-0930h
0° 14′ S. 127° 36′ E.
Depth: 610 m. Wind: N 1.

m	t	S	O_2
0	29,1	32,75	—
20	28,75	32,97	4,84
40	27,92	33,01	4,70
60	26,46	33,24	(5,06)
80	25,36	33,37	3,87
100	23,59	34,38	3,57
120	21,93	34,43	3,47
140	20,86	34,54	3,46
160	19,10	34,56	3,30
180	17,81	34,54	3,27
200	16,94	34,58	3,17
250	12,82	34,60	2,87
370	10,04	34,60	2,63
420	9,76	34,61	2,55
470	9,57	34,61	2,62
520	9,43	34,56	2,57
570	9,27	34,54	2,54
600	9,23	34,56	2,62

Station 25. 24-6-1956 1200-1330h
0° 33′ S. 127° 48′ E.
Depth: > 2000 m. Wind: N 1

m	t	S	O_2
0	29,4	33,93	—
20	28,61	33,91	5,10
40	28,26	33,95	4,98
60	27,23	34,00	4,75
80	26,19	34,14	4,25
100	24,08	34,25	4,09
120	22,08	34,43	3,69
140	21,29	34,45	3,52
160	19,54	34,52	3,39
180	17,28	34,61	3,19
200	16,16	34,67	3,20
250	14,56	34,67	3,17
300	12,54	34,67	3,01
400	9,05	34,61	2,76
500	8,38	34,60	2,83
600	8,19	34,60	2,64
670	8,12	34,61	2,84
765	8,08	34,63	2,75
860	8,01	34,61	2,66
960	8,01	34,65	2,63
1060	8,00	34,65	2,55
1160	7,97	34,65	2,59

Station 26. 24-6-1956 1600-1800h
0° 57′ S. 127° 52′ E.
Depth: 1500 m. Wind: W 2.

m	t	S	O_2
0	28,0	32,75	—
20	29,07	34,18	4,79
60	28,72	34,58	4,73
80	28,11	34,83	4,48
100	27,36	34,87	4,47
120	24,53	34,92	3,81
140	22,32	34,96	3,45
160	20,93	34,90	3,44

180	19,43	34,94	3,42
200	18,54	34,90	3,28
250	15,10	34,69	3,21
300	12,68	34,65	2,97
400	9,93	34,61	2,86
500	8,11	34,56	2,78
600	7,32	34,56	2,81
800	5,82	34,56	2,64
980	5,00	34,60	(2,94)
1070	4,34	34,60	2,77
1170	3,78	34,60	2,94

Station 27. 25-6-1956 0530-0700h
2° 00′ S. 127° 00′ E.
Depth: > 2000 m. Wind: N 1.

m	t	S	O_2
0	28,5	34,16	—
20	28,88	34,25	4,62
55	27,66	34,43	4,41
75	27,08	34,47	4,30
95	25,63	34,65	4,01
110	23,77	34,78	3,68
130	23,25	34,83	3,66
160	22,90	34,87	3,58
180	21,49	34,78	3,41
200	19,15	34,76	3,28
250	15,05	34,61	2,89
300	11,63	34,63	2,80
400	9,23	34,60	2,68
500	7,76	34,63	2,67
600	7,10	34,60	2,67
800	5,72	34,60	2,71
1000	4,53	34,60	2,67
1100	4,29	34,60	2,54
1200	4,04	34,61	2,71

Station 28. 25-6-1956 1800-1930h
3° 32′ S. 127° 38′ E.
Depth: > 3000 m. Wind: 0

m	t	S	O_2
0	29,0	34,40	—
20	28,60	34,36	4,92
60	27,66	34,61	4,62
80	26,98	34,69	4,53
100	24,93	34,65	4,29
120	24,12	34,78	4,26
140	21,68	34,83	(4,25)
160	19,66	34,69	3,46
180	18,19	34,72	3,36
200	16,63	34,69	3,15
250	12,49	34,65	2,97
300	10,33	34,61	2,74
400	8,72	34,65	2,68
500	8,04	34,61	2,71
600	7,12	34,61	2,57
800	5,85	34,61	2,48
1000	4,83	34,61	2,31
1100	4,63	34,61	2,51
1200	4,43	34,61	2,81

Station 29. 28-6-1956 1530h
3° 39′ S. 128° 12′ E.
Depth: 38 m. Wind: 0

m	t	S	O_2
10	28,50	34,13	4,54
15	28,28	34,22	4,25
20	27,67	34,29	3,19
25	27,41	34,29	2,66
30	27,36	34,29	2,35
35	27,11	34,29	2,59

Station 30. 30-6-1956 1600-1730h
2° 55′ S. 127° 26′ E.
Depth: > 2000 m. Wind: S 2

m	t	S	O_2
0	29,2	34,70	—
20	28,99	34,60	4,57
60	28,34	34,92	4,14
80	28,32	34,96	4,47
100	27,62	34,99	4,06
120	26,87	35,03	3,81
140	25,90	35,08	3,69
160	22,95	35,08	3,31
180	22,23	34,99	3,36
200	20,44	34,99	3,11
250	16,77	34,74	2,84
300	13,00	34,70	2,75
380	10,44	34,70	2,71
470	8,57	34,70	2,34
565	7,21	—	—
760	6,58	34,58	2,46
955	4,87	34,63	2,49
1050	4,59	34,65	2,45
1140	4,34	34,69	2,44

Station 31. 1-7-1956 0230-0400h
1° 45′ S. 128° 12′ E.
Depth: 1600 m. Wind: SW 3

m	t	S	O_2
0	28,3	34,27	—
20	28,92	34,14	4,42
60	27,70	34,72	4,04
80	26,72	34,81	3,79
100	25,71	34,96	3,58
120	24,98	34,96	3,71
140	22,60	34,97	3,48
160	17,56	34,76	3,02
180	16,95	—	—
200	16,04	34,74	2,85
250	14,97	—	—
300	13,41	34,72	2,85
400	9,85	34,65	2,58
540	7,97	34,61	2,41
640	6,80	34,61	—
840	5,40	34,61	2,45
1050	4,29	34,60	—
1160	4,09	34,58	2,40
1260	3,83	34,63	2,32

Station 32, 1-7-1956 1500-1700h
0° 12′ S. 128° 49′ E.
Depth: > 2000 m. Wind: W 3

m	t	S	O_2
0	28,9	34,70	—
20	28,95	34,74	5,34
60	28,89	34,79	5,04
80	28,69	34,85	5,17
100	27,96	34,94	4,62
120	26,38	34,99	3,87
140	25,43	35,10	3,51
160	20,92	35,10	3,45
180	18,50	34,99	3,15
200	16,97	34,87	3,02
250	14,48	34,83	(3,32)
300	12,98	34,76	3,20
400	9,73	34,65	—
480	8,35	34,65	3,48
570	8,34	34,67	3,21
740	8,06	34,65	3,31
910	7,92	34,65	3,22
1000	7,90	34,67	3,17
1100	7,90	34,65	3,08

Station 33. 2-7-1956 0930-1100h
0° 51′ N. 128° 46′ E.
Depth: 1200 m. Wind: SW 1

m	t	S	O_2
0	29,0	34,92	—
20	29,11	34,87	4,62
60	28,10	35,21	4,46
80	27,85	35,23	4,02
100	26,94	35,35	3,85
120	26,00	35,44	3,87
140	24,20	35,48	3,37
160	23,27	35,44	3,20
180	21,57	35,37	3,21
200	19,91	35,23	3,12
250	14,41	34,69	3,15
300	12,00	34,65	3,31
400	9,00	34,63	2,94
500	8,09	34,65	2,83
600	7,02	34,56	2,75
800	5,77	34,56	2,72
1000	4,63	34,56	2,60
1100	4,21	34,60	2,56

Station 34. 2-7-1956 1630-1800h
1° 43′ N. 128° 41′ E.
Depth: > 1300 m. Wind: W 2

m	t	S	O_2
0	28,3	34,85	—
20	29,17	34,78	4,75
60	28,33	35,23	4,44
80	27,96	35,35	4,02
100	27,60	35,35	3,77
130	26,38	35,46	3,59
160	22,06	35,35	3,24
180	20,63	35,26	3,19
200	19,29	35,08	3,26
250	13,77	34,58	3,14
300	11,97	34,56	3,05
400	9,23	34,61	2,65
470	8,36	34,58	2,55
570	7,41	34,56	2,59
770	6,05	34,58	2,68
970	4,65	34,58	2,48
1070	4,18	34,61	2,46
1170	3,76	34,60	2,36